Frederick, R. A., Ligrani, P. M., and Thomas, D. L., "Propulsion Research and Academic Programs at the University of Alabama in Huntsville," 53rd AIAA/SAE/ASEE Joint Propulsion Conference, AIAA Propulsion and Energy Forum, (AIAA 2017-4801)

Propulsion Research and Academic Programs at the University of Alabama in Huntsville

Robert A. Frederick, Jr.[1] Phillip M. Ligrani[2] and L. Dale Thomas[3]

UAH Propulsion Research Center, Huntsville, Alabama, 35899

The UAH Propulsion Research Center (PRC) is beginning its 26th year at the University of Alabama in Huntsville (UAH). The mission of the Propulsion Research Center is to provide an environment that connects the academic research community with the needs and concerns of the propulsion community while promoting an interdisciplinary approach to solving propulsion problems. This paper describes highlights from the research and academic programs associated with the center over the past eighteen months. Academic highlights include the offering of new graduate courses in liquid rocket engineering and solid rocket combustion instability. Research highlights include a new supersonic wind tunnel capability and a new program in nuclear thermal propulsion systems engineering. In the 2016 fiscal year, total research expenditures rose to $1.563 million and four Ph.D., eleven master's students, and numerous undergraduate students obtained degrees in conjunction with the center. The center continues to be a resource for both fundamental and applied research as well as a significant contributor to workforce development in the propulsion and energy field.

I. Introduction

THE Propulsion Research Center (PRC) celebrated its 25th year as a University of Alabama in Huntsville (UAH) research organization in 2016. In 2005, Drs. Hawk and Frederick wrote a summary of the activities of the first thirteen years of the UAH Propulsion Research Center.[1] In 2016, Dr. Frederick wrote a summary of student graduation rates, funded research programs, academic programs, and the laboratory capabilities that have developed over the first twenty-five years of the PRC.[2] This paper will highlight progress from the past eighteen months regarding the academic and research programs of the UAH Propulsion Research Center.

[1] Professor of Mechanical & Aerospace Engineering /Director of the Propulsion Research Center, Department of Mechanical & Aerospace Engineering , 301 Sparkman Drive, Olin B. King Technology Hall, Room S226, Huntsville, AL 35899, and AIAA Associate Fellow.

[2] Professor of Mechanical & Aerospace Engineering /Eminent Scholar of Propulsion, Department of Mechanical & Aerospace Engineering , 301 Sparkman Drive, Olin B. King Technology Hall, Room S236, Huntsville, AL 35899, and AIAA Senior Member.

[3] Professor of Industrial and Systems Engineering/Eminent Scholar of Systems Engineering, Department of Industrial and Systems Engineering, 301 Sparkman Drive Olin B. King Technology Hall, Room N151, Huntsville, AL 35899, and AIAA Senior Member.

A. PRC Mission and Strategy

The mission of the PRC is to provide an environment that connects the academic research community with the needs and concerns of the propulsion community, while promoting an interdisciplinary approach to solving propulsion problems. Collaborating individuals and groups are part of the PRC's research goals. This mission is accomplished though cooperation with researchers from government laboratories, other universities, and the aerospace industry. The result of this environment is leading-edge research and scholarly activity in the pursuit of advanced technologies and their applications.

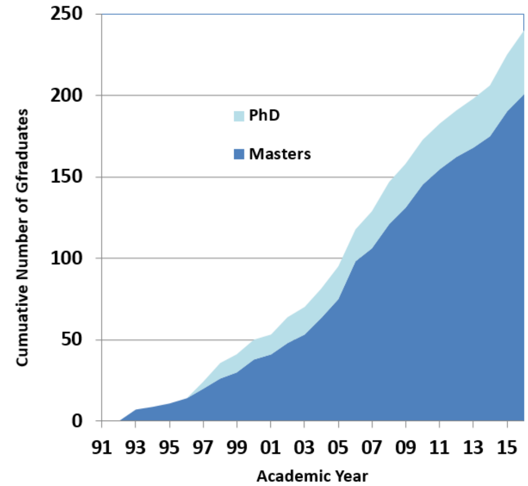

Figure 1. Cumulative Production of Advanced Degrees Associated the PRC.

B. Overall Metrics

Figure 1 shows the cumulative production of advanced degrees from students associated with the Propulsion Research Center from its inception in 1991 to 2017. The total master's degree production has now surpassed 200 and the total Ph.D. production is approaching 40. During the calendar year of 2016, eleven master's students and four Ph.D. students[3-6] completed advanced degrees while working on PRC research.

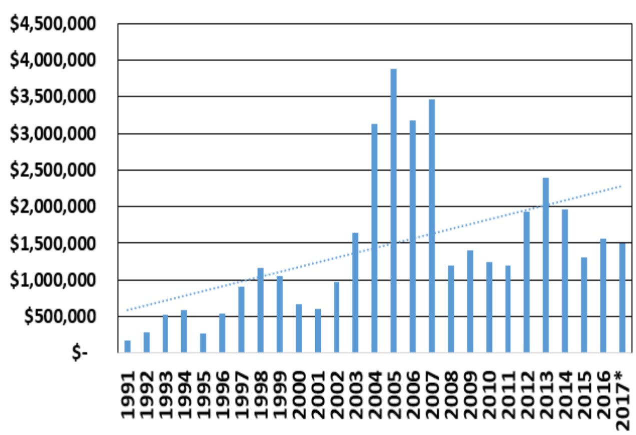

Figure 2. Annual PRC Research Expenditures by FY. *2017 is an Estimate.

Most of the students who receive advanced degrees are in the UAH School of Mechanical & Aerospace Engineering (MAE).

UAH offers advanced degrees in Mechanical Engineering & Aerospace Systems Engineering. Students in other disciplines, such as Chemical Engineering, Physics, Chemistry, and Industrial and Systems Engineering, often do work leading to advanced degrees in partnership with the PRC.

Students are awarded degrees from their home academic departments. The PRC provides an environment for research teams to form and complete research programs that lead to advanced degrees.

Figure 2 shows the annual research expenditures for the Propulsion Research Center since its inception in 1991 to an estimation of 2017. The average annual expenditure level of the entire period is $1.4 million dollars per year. The peak funding occurred in FY 04 at $3.9 million. These were years (2004-2007) where significant new capabilities and infrastructure were supported. The periodic "surges" in funding generally represent the growth and completion of significant efforts with a particular sponsor.

The two most recently completed fiscal years show an increase in funding levels. Total expenditures rose from $1.308 million (FY 15) to $1.563 million (FY 16). The research expenditure numbers do not include cost shares, internal university administrative funds, or UAH Foundation investments into the PRC.

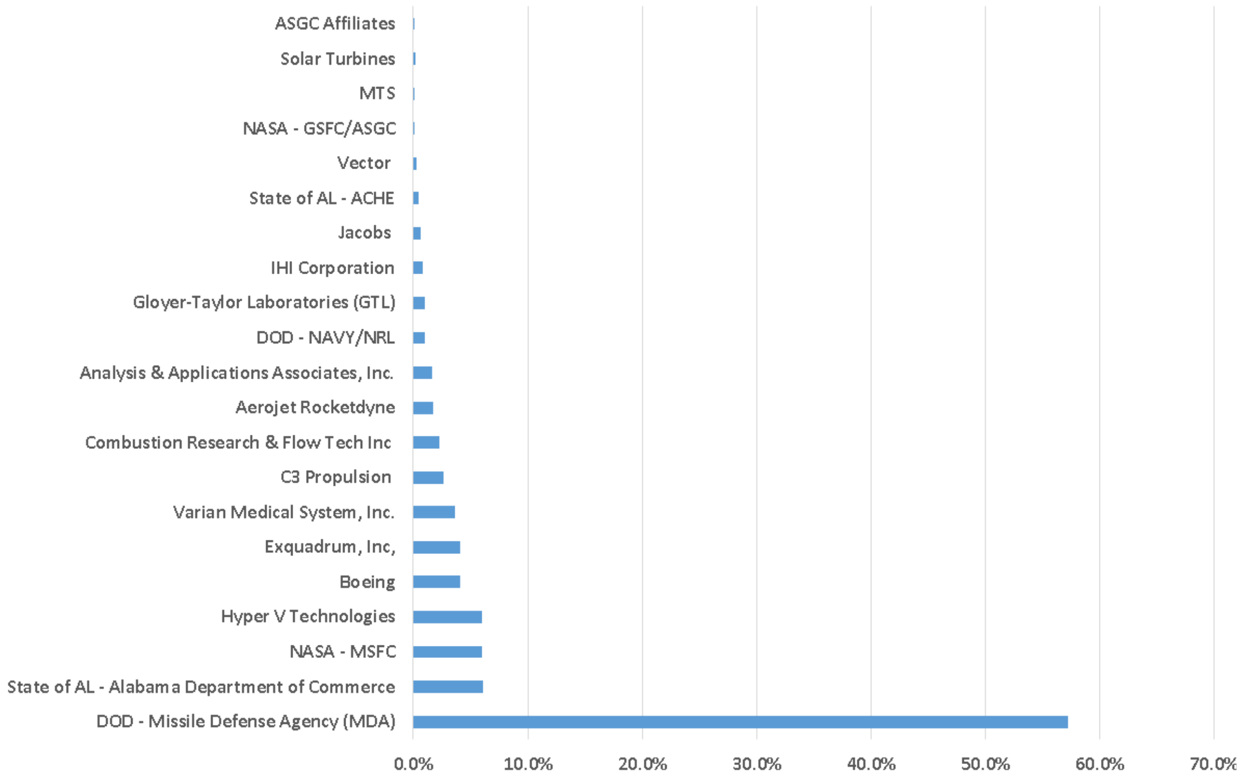

Figure 3. Distribution of Research Expedintures by Sponsor from Oct. 2014-July 2017

C. Current Research Programs

This section highlights the sponsors and levels of funding from FY 15 to the present. Figure 3 shows the cumulative expenditures distributed over twenty-one sponsoring agencies for this time period. The Missile Defense Agency (MDA) work performed by the PRC involves independent assessment of propulsion and energy technologies and the work supports a multi-disciplinary team of faculty, staff, and graduate students. MDA is currently our “anchor tenant” and provides over 50% of the funds expended. The other twenty projects involve state agencies, NASA, aerospace companies, small businesses, and private companies. In FY 16, two new sponsors funded research at the PRC: Solar Turbines, Inc. in the area of air breathing engines, at an anticipated total level of $966,668 from Oct. 2017 to 2022, and Manufacturing Technical Solutions, Inc. (MTS) in the area of Nuclear Thermal Propulsion System Studies. Example research program highlights are summarized in later Section III of this paper.

II. Academic Infrastructure

A. Mechanical & Aerospace Engineering

The Department of Mechanical & Aerospace Engineering provides the majority of the faculty and students that participate in PRC research activities. The MAE Department offers Bachelors of Science Programs in Aerospace Engineering & Mechanical Engineering accredited by the Accreditation Board for Engineering and Technology, Inc.

(ABET). At the graduate level, the MAE department offers Master's and Ph.D. Programs in Aerospace Systems Engineering & Mechanical Engineering.

> The mission of the UAH Department of Mechanical & Aerospace Engineering (MAE) is to provide undergraduate and graduate education, research, and public service in the Mechanical & Aerospace Engineering disciplines and to support the Mechanical & Aerospace Engineering needs of Huntsville, the State of Alabama, the region, our nation, and the international community.[4]

The undergraduate program had a remarkable growth rate last year, expanding from 950 undergraduates in academic year (AY) 15-16 to 1,068 in AY 16-17 with an anticipated 1,200 students in the fall of 2017. The Aerospace portion at the undergraduate level has concurrently grown from about one-third to one-half of the undergraduate population. The graduate program decreased from 170 students in AY 15-16 to 150 students in AY 16-17. This decline comes in part from a decrease in part-time students alongside a relative increase in full-time students.

The MAE Department added two new tenure-track faculty in AY 15-116, bringing the total to twenty tenured and tenure-track faculty; the first new faculty member is in the area of spacecraft dynamics and the second is in the area of advanced power systems. The MAE department also added one lecturer in AY 15-16, bringing the total to five full-time lecturers to assist with the growing undergraduate population. Several part-time instructors also help carry the teaching load for the department.

B. Propulsion-Related Courses

Table 1 shows several propulsion-related classes offered at UAH. The dual-level courses allow undergraduate and graduate students to learn together. Undergraduates at UAH can also participate in a Joint Undergraduate Master's Program (JUMP) in which they can earn both undergraduate and graduate credit for taking dual-level classes.

In the summer of 2016, the PRC combined resources with the UAH College of Engineering and the UAH College of Professional and Continuing Studies to offer two new courses in Aerospace Engineering (Propulsion): MAE 695 – Solid Rocket Combustion Instability and MAE 695 – Liquid Rocket Engineering. Thirty-five UAH graduate engineering students and fifteen professional development students participated in the lectures. Professional development students from South Africa, Europe, and Canada, as well as students employed by NASA and John Hopkins University, participated in the courses.

The lectures were completed in a five-day intensive format with professional development and graduate students present for all classroom lectures. The UAH

Table 1. UAH Undergraduate and Graduate (Dual Level) Academic Courses Related to Propulsion and Energy

Dual-Level Undergrad/Graduate	AY 15-16	AY 16-17
MAE 343 – Compressible Aerodynamics		79
MAE 420/520 – Compressible Aero	49	
MAE 440/540 – Rocket Propulsion I	55	34
MAE 441/541 – Airbreathing Propulsion	17	38
MAE 444/544 – Intro. To Electric Prop.	22	0
MAE 468/568 – Eleme. of Spacecraft Des.	48	61
MAE 493/593 – Rocket Design	28	19
MAE 495/595 – Intro. To Nuclear Prop	0	21
TOTAL	**219**	**252**
MAE Graduate-Level	**AY 15-16**	**AY 16-17**
MAE 620 – Compressible Flow	21	11
MAE 640 – Rocket Propulsion II	0	21
MAE 633 – Tactical Missile Design I	0	0
MAE 644 – Adv. Solid Rocket Propulsion	22	0
MAE 645 – Combustion I	6	0
MAE 681 – Missile Trajectory Analysis	0	0
MAE 745 – Combustion II	0	0
MAE 795 – ST: Intro to Fusion Propulsion;	11	0
MAE 695/795 – ST Adv. Readings in Prop.	7	3
MAE 695 – Comb. Instability in Solid Rockets	15	0
MAE 695 – Liquid Rocket Engineering	20	0
TOTAL	**102**	**35**

[4] http://www.uah.edu/eng/departments/mae/mission-statement

graduate engineering students then completed additional academic requirements for the courses by meeting for an additional three weeks with an instructor. The lectures from these courses were recorded and are currently offered online for professional development credit as part of a Professional Certificate Programs in Rocket Propulsion.

These new offerings increase UAH's presence as a national leader in aerospace engineering, professional development, and graduate education in propulsion-related engineering topics.

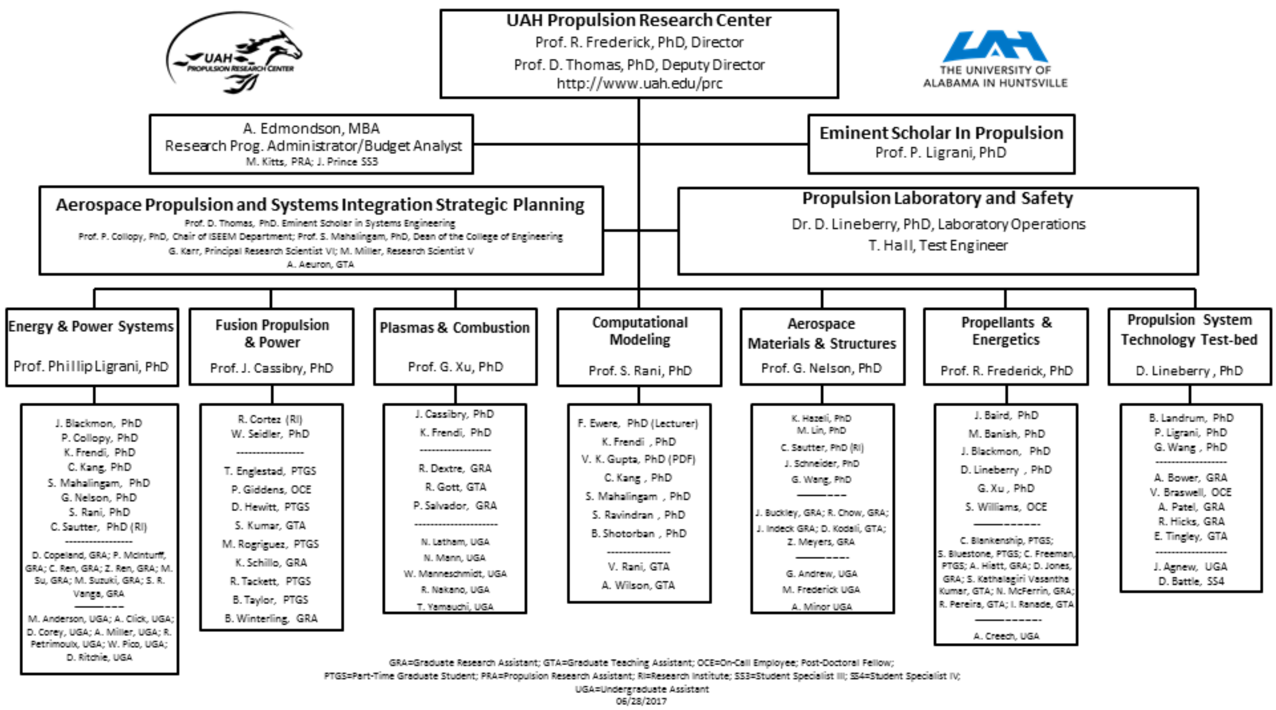

Figure 4. The PRC Organization Chart.

III. Research Highlights

Figure 4 shows the current PRC organization chart. Each box represents a functional area in the organization. Currently, there are over 100 faculty, staff, and students associated with PRC research activities. The overall activities are managed by a director who is supported by staff that manage fiscal programs, advise in technical matters, and oversee laboratory operations. The bottom row of the organization chart shows seven topic areas from Energy and Power Systems to Propulsion Systems Technology Test-bed. Each of these areas has a lead contact. The names beneath these boxes show participating faculty and staff, graduates students, and undergraduates students who are active in each area.

This past year, Dr. L. Dale Thomas was appointed as the Deputy Director of the Propulsion Research Center. He has over thirty years of systems engineering and propulsion experience at NASA. Dr. Thomas is leading propulsion systems engineering research and strategic planning activities. He joined UAH in 2015 and was named the Eminent Scholar in Systems Engineering and a Professor of Industrial and Systems Engineering.

The next sections will briefly describe some of the current activities and capabilities and are presented using the areas shown in the organizational chart.

C. Propulsion and Systems Integration

The mission of the UAH Propulsion Research Center is the advancement of basic science and technology development related to propulsion and energy. These advances, while in and of themselves constituting complex and challenging endeavors, are not ends unto themselves. Success in propulsion research is ultimately characterized by infusion of a scientific principle or a matured technology into a system. A NASA internal study found that technology infusion challenges (not technology readiness challenges) most often hinder successful application of advanced technologies in NASA mission systems.[7] These challenges most often take the form of integration roadblocks at the architectural or system level.[8] NASA recognizes the criticality of integration roadblocks as evidenced by the following excerpt from the 2015 NASA Technology Roadmap:

> Recent experiences with deep-space systems have highlighted cost growth issues during integration, testing, and operations. These include changes to the design late in the life cycle, often resulting in a ripple effect of additional changes in other areas, unexpected results during testing due to unplanned interaction of fault responses, and operational limitations placed on the spacecraft based on how the system was tested, in order to 'fly-as-you-test.' These issues cause cost and schedule growth during system development.[9]

Efforts are underway at the PRC and Complex System Integration Lab (CSIL), shown in Fig. 5, to apply Model Based Systems Engineering (MBSE) to advanced propulsion systems integration as a method to address the propulsion technology infusion problem.

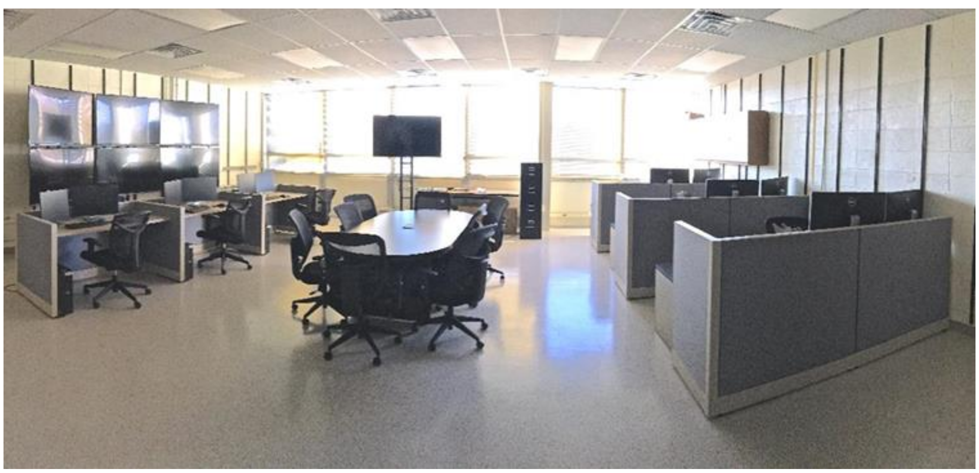

Figure 5. Complex System Integration Lab (CSIL).

A Nuclear Thermal Propulsion (NTP) space transportation vehicle for human exploration beyond cislunar space is the subject of one study. Although the fundamentals of NTP are well understood and ground test data exist from the Nuclear Engine for Rocket Vehicle Application (NERVA) program in the 1960s, it has never been used in a spaceflight vehicle, nor have any vehicle designs gone beyond the conceptual stage. The Systems Modeling Language (SysML) is employed for this modeling effort to develop an integrated systems model that captures both the structure and behavior of a NTP spaceflight vehicle. The baseline case under consideration is a hot bleed cycle type engine for a mission architecture to Mars employing transfer orbits faster than Hohmann Transfers. In addition to providing an integrated system model of a point design, mathematical models enable derivation of scaling relationships between the NTP system, the flight vehicle, and the orbital mechanics driven by the destination and mission duration.[19] The model, depicted in Fig. 6 and 7, allows elements to be added or replaced as necessary to change the model for increased fidelity calculations or to add new capabilities, such as electricity generation from the nuclear reactor or liquid oxygen augmented thrust. This allows the integrated systems model to start very simple and grow to the requisite complexity. Along the way, MBSE provides the very significant benefit of mutually consistent requirements, system design, and concept of operations – an important consideration in the pre-conceptual studies portion of a life cycle when myriad mission concepts and system trade studies can and typically does lead to gaps and conflicts.[10]

The NTP project serves as a pathfinder for propulsion systems integration utilizing advanced propulsion technologies. For a successful propulsion system development, decisions need to be informed concerning the engineering considerations at both the integrated engine and vehicle level, as the optimal choice at the engine component level may be suboptimal at the integrated level, and in turn differ again at the integrated vehicle level. The focus of this research is to apply MBSE to develop systems engineering models for the engine components, the engine, and vehicle, providing specifications and sensitivities of alternatives to enable determination of an optimal vehicle configuration for a given mission. The advanced propulsion systems integration tools and techniques developed and analyses performed in this research will allow propulsion systems to be realized which incorporate new scientific principles and technologies, and realized more quickly, economically, and reliably at lower risk

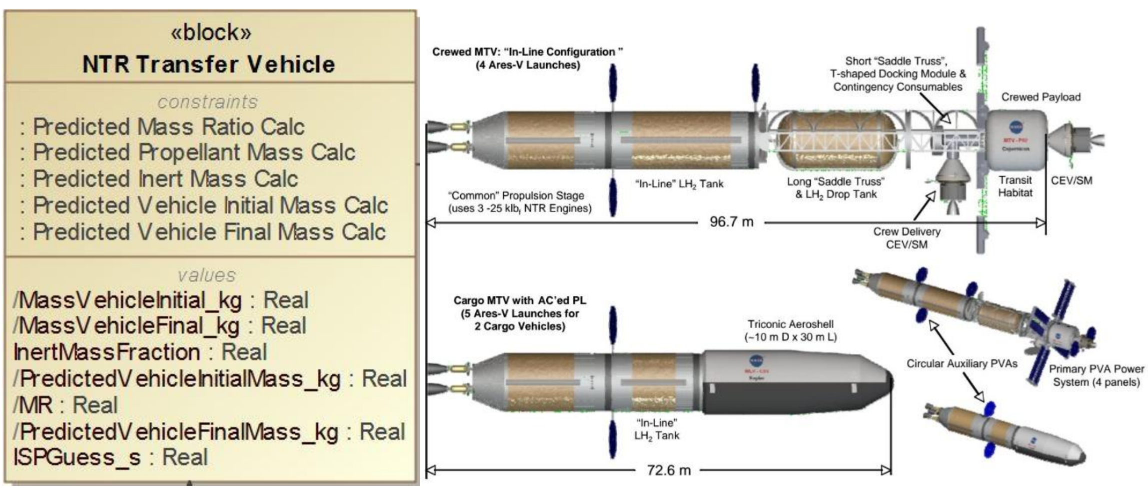

Figure 6. NTR Transfer Vehicle block from the model[10] pictured next to the NTP powered crew and cargo vehicles from NASA DRA 5.[19]

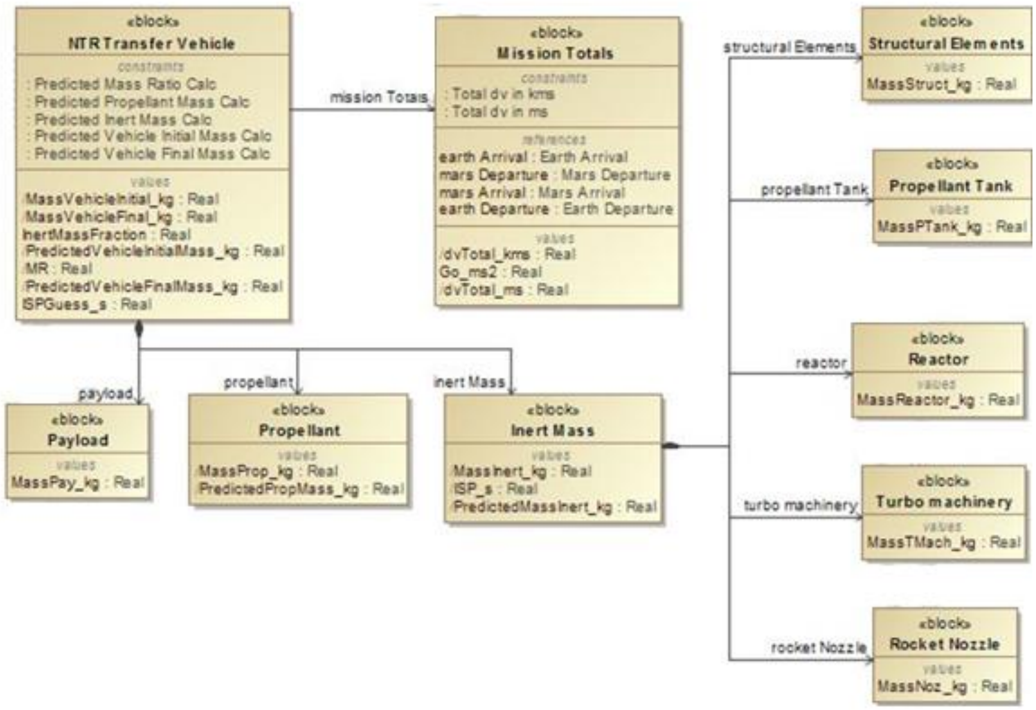

Figure 7. NTR Transfer Vehicle Hierarchy on NTR Block Definition Diagram.[19]**Error! Bookmark not defined.**

D. Propulsion Laboratories

The PRC makes extensive use of laboratories for research programs. Several laboratories are administered and maintained by the PRC at the Propulsion Test Facility the Johnson Research Center, and at other locations around the UAH Campus. PRC-affiliated faculty also complete research projects in their own laboratories on campus and on Redstone Arsenal.

Table 2 is a listing of these laboratories. This year, several upgrades and additions should be noted. The Propulsion Test Facility is undergoing two major upgrades. The Hot Fire Rocket Test Cell is undergoing a $500,000 upgrade to install a larger test stand, an altitude capability, and completely new data acquisition system; more details on this will be reported next year when the work is complete. The Supersonic Wind Tunnel Facility is adding additional test sections and several new large blow down tanks. The Mechanics of Materials under Extreme Conditions Laboratory came online and recently won support to add new instrumentation. The description and use of several of these facilities are described in the following sections.

Table 2. Laboratories Associated with PRC Research

Propulsion Test Facility	**Location**
Hot-Fire Rocket Test Cell (Cryogenic)	UAH Johnson Research Center
Supersonic Wind Tunnel	UAH Johnson Research Center
Johnson Research Center	**Location**
Charger Rocket Works (Student Sounding Rockets)	UAH Johnson Research Center
Injector Spray Facility	UAH Johnson Research Center
Plasma and Electrodynamics Research Lab (PERL)	UAH Johnson Research Center
Thermal Fluids Sciences Lab	UAH Johnson Research Center
Vacuum Chamber Test Lab	UAH Johnson Research Center
OTHER PRC	**Location**
High-Pressure Solid Propellant Lab	Material Science Building
Solar Thermal Lab	Blackmon Hall
Other UAH	**Location**
Adaptive Structures Lab	UAH Technology Hall
Advanced Manufacturing Processes Laboratory or AMPL.	Aerophysics Research Center, Redstone Arsenal
Charger One - Fusion Propulsion	Aerophysics Research Center, Redstone Arsenal
Complex Systems Integration Laboratory (CSIL)	UAH VBH
Mechanics of Materials Under Extreme Environments	UAH Optics Building
Transport, Reaction, and Energy Conversion Lab	UAH Shelby Center

Laboratory safety is always of paramount importance for all activities at the PRC. A five-year, external Process Hazards Analysis (PHA) revalidation was performed on the PRC by Safety Management Services Inc. The PHA was based on evaluation of PRC-provided information and onsite evaluations at UAH on January 24 – 25, 2017. The PHA was tailored to meet requirements of OSHA 29 CFR 1910.119 "*Process Safety Management of Highly Hazardous Chemicals*," and the requirements outlined in DOD 4145.26-M "*DOD Contractor's Safety Manual for Ammunition and Explosives*." Based on the type and complexity of the process, a Failure Modes and Effects Analysis (FMEA) methodology was chosen for this effort. Where deficiencies existed, recommendations were issued to minimize or eliminate the potential risk of identified failure scenarios. PRC leadership reviewed the recommendations and appointed a team to make appropriate improvements and address items provided by this review.

E. Energy and Power Systems

1. Supersonic Flow and Shock Wave Interaction Investigations

This research activity is under the direction of Dr. Ligrani, and is sponsored by (a) the Alabama Innovation Fund of Montgomery, Alabama, (b) the Office of the Vice President for Research and Economic Development of the University of Alabama in Huntsville, Huntsville, Alabama, (c) Endowment Funds of the Eminent Scholar in Propulsion of the University of Alabama in Huntsville, Huntsville, Alabama, and (d) the Arnold Engineering Development Center of Arnold Air Force Base, Tullahoma, Tennessee.

Over the past eighteen months, efforts have been underway within the Propulsion Research Center to develop capabilities to investigate supersonic flows, including topics related to shock wave interactions. To accomplish this objective, four high pressure air storage tanks (donated from the Arnold Engineering and Development Center) have been installed and mounted on a concrete pad. A low-pressure piping and valve system, including an air diverter plenum, regulation valves, and safety devices, has been installed and is operational. The high-pressure valve and piping system is being installed with completion expected by August of 2017. The design of the facility allows the installation and use of three different test sections, installed in a parallel fashion. The supersonic test section includes an inlet duct, supersonic nozzle, supersonic test section, exhaust plenum, instrumentation, and Schlieren flow visualization system. The facility also includes a variety of flow management devices which are installed upstream of the supersonic wind tunnel test section. With the present air supply, and low-pressure piping and valve arrangement, inlet test section Mach numbers up to 3 can be achieved. Future configurations are expected to provide test section Mach numbers as high as 5 or 6. The facility is designed with an inlet supply plenum and an exhaust plenum, just upstream and downstream of the test section, in order to minimize the flow fluctuations and unsteadiness which could propagate from locations, either farther upstream or farther downstream.

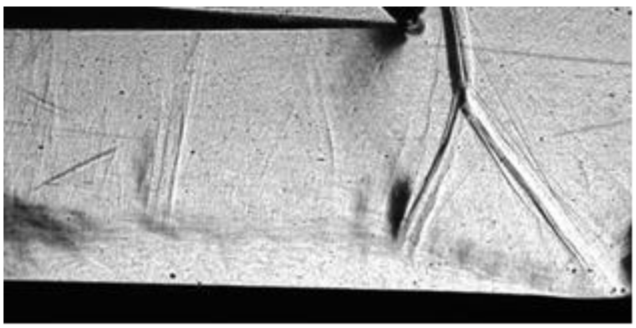

Figure 8. Schlieren flow visualization image showing normal shock wave, including lambda foot, and separated turbulent boundary layer. Flow direction is from right to left. Choking flap is oriented at 3.7 degrees, and test section inlet Mach number is 1.54.

Variations of stagnation pressure, static pressure, and Mach number, measured at the inlet of the supersonic test section, show that, with the presently installed nozzle, the supersonic test section inlet Mach number is about 1.54, and can be maintained at the test section inlet for a period as long as thirty seconds. Testing times up to ten to twelve minutes will be possible, upon installation completion of the high pressure piping and valve system, mentioned above. New Schlieren flow visualization results, obtained using the supersonic wind tunnel test section, are shown in Fig. 8. Here, the Schlieren flow visualization image shows a normal shock wave, including lambda foot, and separated turbulent boundary layer. Flow direction is from right to left. To obtain these data, the choking flap, located within the downstream part of the test section, is set at 3.7 degrees. Note that the different shock wave configurations (i.e. oblique or normal) can be induced by changing the angle of this choking flap.

Ongoing and future research efforts are directed towards unsteady effects in shock wave boundary layer interactions,[11,12] as well as the effects of such interactions on surface heat transfer variations.[13-19]

2. Elastic Turbulence Investigations

This research activity is under the direction of Dr. Ligrani (as co-Principal Investigator), and is sponsored by the U.S. National Science Foundation of Arlington, Virginia. The work is undertaken in collaboration with Professor Robert Handler (also as co-Principal Investigator) of George Mason University of Fairfax, Virginia. Of interest is thermal transport due to elastic turbulence. As such, several different experimental configurations are employed to induce appropriate amounts of fluid strain within controlled environments: Viscous Disk Pump (VDP), Rotational Couette Flow (RCF), and Serpentine Flow (SF).[20-24]

The Viscous Disk Pump or VDP experimental apparatus is composed of a spinning disk and a C-shaped channel with a fluid inlet port and a fluid outlet port, located at the two ends of the C-shaped channel.[20,21] With this device, rotating Couette-type flow is induced within the fluid chamber between the rotating disk and the stationary bottom of the channel. The VDP is employed because magnitudes of shear rate imposed on the flow are readily selected by setting disk rotational speed and the gap height of the flow passage.

To characterize the onset of elastic instabilities within the VDP, relationships provided by McKinley et al.[25] are derived into forms which are applicable to the VDP. The resulting transition relationship is expressed in terms of the Weissenberg number, the Deborah number, and the ratio of viscosities, which are related to relative contributions of the solvent and polymeric components of the fluid. The result obtained with this approach shows a reasonable match to the present elastic instability transition onset conditions from flow visualization results, especially for the higher concentrations of polyacrylamide which are considered.

Variations of convective heat transfer characteristics for the polyacrylamide/sucrose solutions and the Boger solutions[26] are determined from measurements and analysis for VDP disk rotational speeds of 52.3 radians/s, 104.7 radians/s, 157.1 radians/s, and 209.4 radians/s. The resulting spatially-averaged Nusselt numbers increase with disk rotational speed for each polymer concentration employed. When compared for a particular shear rate or disk rotation speed, the minimum Nusselt number is always associated with the pure sucrose solution, which is the Boger fluid. Spatially-averaged Nusselt numbers thus show significant variations as polyacrylamide concentration is changed, which are tied to different extents of elastic turbulence development.[27-32] Associated variations within the viscous disk pump flow passage are thus associated with increased polymer interactions and agitation, and enhanced local mixing,[27-32] which results in overall increases in local and global thermal transport. As such, the elastic turbulence increases heat transfer by approximately 240 percent for the sucrose solution with a 150 ppm polymer concentration (relative to the Boger solution with ρ_c=0 ppm), when compared at the same disk rotational speed.[33,34]

3. Double Wall Cooling Investigations

This research activity is under the direction of Dr. Ligrani, and is sponsored by Solar Turbines, Inc. of San Diego, California. Overall, the project utilizes a facility which is designed to provide full coverage film cooling effectiveness data and impingement cooling effectiveness data, wherein the film cooling flow is supplied using either cross flow,[35,36] impingement flow,[37] or a combination of both together. A sparse effusion hole array is utilized within the investigation. The experimental facility uses three independent flow channels to provide double wall cooling arrangements which model configurations from combustor liner components of gas turbine engines. Included are new experimental data for both the hot/mainstream side, and the cold/cross flow side of the effusion plate. For the effusion cooled/hot surface, presented are spatially-resolved distributions of surface adiabatic film cooling effectiveness, and surface heat transfer coefficients (measured using infrared thermography).[35-37] For the coolant/cross flow/impingement cooled side, presented are spatially-resolved distributions of surface Nusselt numbers (measured using liquid crystal thermography).[35-37] Of primary interest are the effects of impingement jet Reynolds number, effusion blowing ratio, streamwise development, and mainstream Reynolds number.

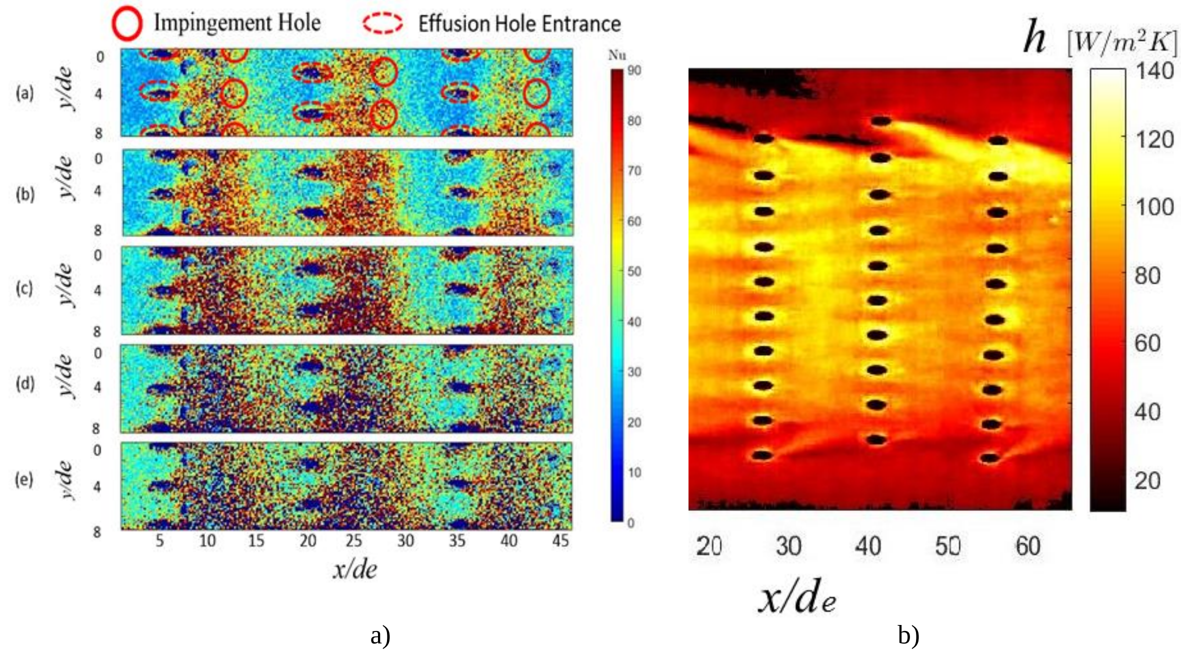

Figure 9. a) Comparison of local, spatially-resolved surface Nusselt number variations for cold side of effusion plate for different blowing ratios BR and mainstream Reynolds number of 142,000-155,000, from Ligrani et al. [37] (a) BR=3.3. (b) BR=4.3. (c) BR=5.5. (d) BR=6.3. (e) BR=7.4.
b) Surface, local heat transfer coefficient variation for hot side of effusion plate for BR=7.4 and mainstream Reynolds number of 142,000, from Ligrani et al. [37]

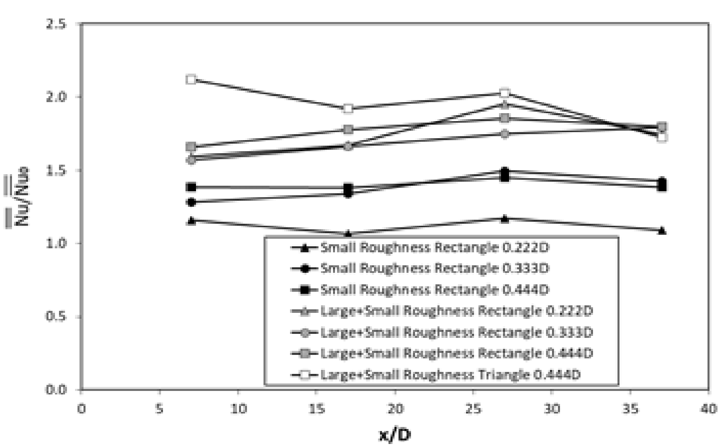

Figure 10. Spatially-Averaged Nusselt Number Ratios for Different Roughness Heights and Different Roughness Configurations. Rej=5000, from Buzzard et al. [38,39]

Experimental data are given for a ratio of jet-to-target plate distance to effusion hole diameter of 14, impingement plate thickness of 3.0 effusion hole diameters, and spanwise and streamwise impingement hole spacing such that coolant jet hole centerlines are located midway between individual effusion hole entrances. For the effusion cooling, streamwise hole spacing and spanwise hole spacing (normalized by effusion hole diameter) are 15 and 4, respectively. Effusion hole angle is 25 degrees, and effusion plate thickness is 3.0 effusion hole diameters. Considered are overall effusion blowing ratios from 3.3 to 7.4, with subsonic, incompressible flow. As such, the effusion film is turbulent for all experimental conditions investigated. Note that velocity of the freestream flow which is adjacent to the effusion cooled boundary layer can be set to be approximately constant with streamwise distance or can be set to increase with streamwise distance, as a result of a favorable streamwise pressure gradient.

Examples of spatially-resolved experimental results are given in Fig. 9. Figure 9 a) provides a comparison of local, spatially-resolved surface Nusselt number variations for the coolant / cross flow side of the effusion plate, for different blowing ratios for a mainstream Reynolds number of 142,000-155,000. Here, data are given for blowing ratio BR values of 3.3, 4.3, 5.5, 6.3, and 7.4. Note that normalized streamwise location x/de = 0 is defined at the upstream edge of the area of present spatially-resolved measurements. Also included within Fig. 9 a) are locations of the impingement holes as well as the effusion hole entrances.

According to the results within Fig. 9 a), regardless of the value of blowing ratio BR, the highest local Nusselt numbers are present at smaller x/de locations, relative to the locations of the impingement hole centerlines. Such Nusselt number augmentation regions are associated with impingement jet stagnation locations, which are positioned at different x/de locations, relative to the impingement holes. This is because of turning and re-direction of the impingement jets as they cross the impingement passage. The re-direction is a result of the static pressure variations within the passage, with lowest values near the entrances of the effusion holes. With this physical situation, coolant within impingement jets exits the impingement holes, turns to smaller x/de locations, and then impacts upon the coolant side of the effusion plate. Afterwards, the coolant is then re-directed along the plate surface. Afterwards, it enters into individual effusion holes, which are also located at smaller x/de locations, relative to adjacent impingement hole locations.

Figure 9 b) gives surface, local heat transfer coefficient variations in dimensional form for BR=7.4 and a mainstream Reynolds number of 142,000. Here, heat transfer coefficients range from approximately 20 W/m^2K to 140 W/m^2K along the test surface. Higher heat transfer coefficient values are generally observed just upstream, around, and along a trajectory downstream of each hole. Lower heat transfer coefficient values are generally present away from the holes. These variations are tied to jet mixing, vortex development around jet coolant concentrations, increased shear near jet edges, and the resulting augmentations of local three-dimensional turbulent transport.

4. Surface Roughness Effects on Impingement Array Surface Heat Transfer

This research activity is under the direction of Dr. Ligrani, and is sponsored by IHI Corp. of Tokyo and Yokohama, Japan. Overall, the focus of the effort is fundamental understanding of thermal transport, and heat transfer phenomena, as altered by impingement array jets as they impact upon different target surface roughness arrangements. Applications are varied, and include electronic cooling, electronic component chip cooling, heat exchangers, utility gas turbine engines employed for power generation, micro-fluidic devices which are employed within electronic components, as well as a variety of other heat transfer augmentation devices.

A variety of different surface roughness configurations are considered, along with a smooth target plate, which is employed to provide baseline comparison data. Included are surface arrays of small rectangular roughness,[38,39] small triangle roughness[40,41] and small cylinder roughness,[42,43] as well as surface arrays of small roughness, employed in conjunction with large pin roughness.[38-43] Considered are a variety of different roughness shapes, different roughness configurations, different roughness heights, and different values of *Rej*, impingement jet Reynolds number.

An example of spatially-averaged surface Nusselt number ratios are given in Fig. 10, from Buzzard et al.[38,39] Here, the baseline Nusselt numbers used for normalization of these results are obtained with impingement cooling applied to smooth target surfaces at the same experimental conditions. Note that no other baseline condition is appropriate for normalization of these impingement cooling results. The turbulent data in Fig. 10 are given for rectangle small roughness, both with and without large pin roughness. Here, the jet Reynolds number is 5000. Within this figure, spatially-averaged Nusselt number ratios generally increase at each *x/D* location, as small roughness height increases (from 0.222D to 0.333D to 0.444D, where D is impingement hole diameter), and as large pins are added to the configurations. Such behavior results from increased local mixing and local turbulent transport, as roughness elements become higher and/or more numerous. Also important is the increase in wetted surface area, relative to a smooth target surface, which results from the addition of the different roughness elements. Note that the highest spatially-averaged Nusselt number ratios are present for a surface array of small triangle roughness with 0.444D height, with large pin roughness. With this arrangement spatially-averaged Nusselt number ratios are as high as 2.2.[38,39]

5. Internal Passage Heat Transfer Augmentation Methods and Associated Unsteady Flow Structural Characteristics

This research activity is a collaborative effort between Dr. Ligrani, Professor Jing Ren, Professor Hongde Jiang, and associated graduate students of the Institute for Gas Turbines of Beijing Tsinghua University of the P. R. China. Of interest is experimental and numerical investigation of unsteady impingement cooling within a blade leading edge passage,[44] as well as unsteady structure and development of both laminar and turbulent impingement jets, including Kelvin-Helmholtz vortex development.[45,46] Different turbulence models are also assessed in regard to predictions of narrow passage flows with impingement jets,[47] and with pin fin arrays.[48] Other recent efforts address effects of Reynolds number, hole spacing, jet-to-target distance, and hole inclination angle on the convective heat transfer performance of an impinging jet array over Reynolds numbers from 5,000 to 25,000.[49] Streamwise and spanwise jet-to-jet spacing 4D-8D and jet-to-target plate distance of 0.75D to 3D are employed, where D is impingement hole diameter. Also investigated is the effect on the heat transfer coefficient of hole inclination angle θ, which ranges from 0° to 40°.

6. Second Law Losses around a Turbine Guide Vane

This research activity is a collaborative effort between Dr. Ligrani and Professor Bernhard Weigand, and associated graduate students, of the Institute of Aerospace Thermodynamics at the University of Stuttgart in Germany. Of interest is the determination of entropy production from the flow field around a turbine guide vane, and the numerical simulation of this flow field by means of Computational Fluid Dynamics (CFD).[50] These CFD simulations are based upon RANS, the Reynolds Averaged Navier-Stokes equations, and are carried out using ANSYS CFX-14.0 and the Shear Stress Transport (SST) turbulence model. The flows around the vane from experimental investigation are simulated for three vane Mach number distributions, each of which is characterized by a different vane trailing edge Mach number. To obtain entropy production from the numerical flow field, two approaches based on second law analysis are utilized: a conventional and a differential one. The conventional approach describes global entropy production between two thermodynamic states by calculating it from the total pressure loss inherent to irreversible processes.[51] The differential approach makes use of the entropy transport equation and yields local entropy production rates along pathlines directly from local flow field variables predicted by the CFD. Global entropy production is then determined by integrating local exergy destruction rates along pathlines, with respect to time.[50]

7. Unsteady Milliscale Impingement Jets and Associated Vortices for Surface Heat Transfer Augmentation

This research activity, involving Dr. Ligrani, is in collaboration with Professor Dae Hee Lee, and associated graduate students, of the Department of Mechanical and Automotive Engineering of Inje University, located in South Korea. Of interest is jet impingement cooling of electronic chips, which are equipped with different cylindrical pedestal fin arrangements.[52,53] More recently, confined, milliscale unsteady laminar impinging slot jets are investigated as they influence surface Nusselt numbers with constant surface heat flux and constant surface temperature thermal boundary conditions.[54-56] Also considered are effects of confined impinging slot jets on heat transfer to concave and convex surfaces.[57] The structure of the associated vortices, which form within the shear layers, which are adjacent to the slot jets, are investigated using flow visualizations.[58] From these data, flow characteristics of confined, laminar milliscale slot jets are revealed, as the jets impinge upon a flat target plate, with a fully-developed velocity profile at the nozzle exit. The effects of Reynolds number and normalized nozzle-to-plate distance are considered for specific values of nozzle width. Transition from a stable symmetric jet to an unsteady oscillating jet is observed as the Reynolds number increases (with normalized nozzle-to-plate distance constant), where the Reynolds number associated with this transition decreases as the normalized nozzle-to-plate distance increases. Instantaneous visualizations also show unsteady lateral distortions of jet columns at experimental conditions corresponding to the presence of continuous sinusoidal oscillations, intermittent oscillating motion of the jet column, and jet flow fluctuation/flapping motion. Associated jet and vortex structural changes are determined for different modes of unsteadiness,[58] including characterization of jet column unsteadiness using jet column oscillation frequency, and lateral and streamwise extents of jet distortion.[58]

8. Dean Flow Dynamics and Cell Separations in Low-Aspect Ratio Spiral Microchannels

This research activity, involving Dr. Ligrani, is in collaboration with Professor Ian Papautsky, and associated graduate students, of the BioMicroSystems Laboratory of the University of Cincinnati. Of interest are spiral inertial microfluidic devices for continuous blood cell separations,[59] as well as microfluidic inertial, continuous SPLITT, and field-flow fractionation technologies for separations of whole blood components.[60] More recently, secondary Dean vortices[61,62] in spiral microchannels are investigated,[63] and used to advantage for cell separations.[64] Recent attention is focused on curvilinear channel geometries because of the presence of secondary flows, which, with appropriate configurations and flow conditions, can be employed to promote cell separations. In general, such devices are designed with the assumption that there are two counter rotating Dean vortices, present in the curved rectangular channels, which exist in the state of steady rotation and amplitude. Within the collaborative effort, these secondary Dean flows are investigated in low aspect ratio spiral rectangular microchannels, including their development with respect to the channel aspect ratio and Dean number. Dean vortex flows are shown to be present when Dean number exceeds a critical value. Multiple vortex vortices (>2) are also considered, including their effects on particle and cell focusing. Overall, results from these studies offer new insights into secondary flow instabilities for low-aspect ratio, spiral microchannels, with improved flow models for design of more precise and efficient microfluidic devices for applications, which include cell sorting and micromixing.[63,64]

F. Fusion Propulsion Systems

Fission/fusion hybrid[65] and pulsed fusion propulsion,[66] have been shown to significantly reduce the trip times for space travel. The specific approach being pursued at UAH PRC is called “z-pinch.” Reviews of this topic can be found in Refs. 67 and 68. We are specifically pursuing solid density z-pinch implosion with fuel cycles that do not require cryogenic storage.

The fusion propulsion research underway at UAH utilizes Charger 1, a 550 kilojoule (kJ), 3 Terawatt (TW) pulsed power machine as depicted in Fig. 11. Charger 1 is located on the Redstone Arsenal at the Aerophysics Research Center (ARC) shown in Fig. 12. Charger 1 was developed by L-3 Communications Pulsed Sciences division on a Defense Threat Reduction Agency (DTRA) contract, and it was originally used for nuclear weapons effects testing. UAH acquired the machine in May of 2012, with assistance from the Boeing Company.

Since then, UAH has worked regularly with the NASA Marshall Space Flight Center, Boeing, and the Y-12 National Security Complex to make Charger 1 operational to conduct advanced propulsion experiments. The Defense Threat Reduction Agency (DTRA) spent $850,000 to safely dismantle Charger 1 to have it shipped to Huntsville from its original location in San Leandro, CA. UAH won a $300,000 award from the state of Alabama through its innovation fund to help towards refurbishing and assembling the main sections of the machine. This included rebuilding and replacement over 200 custom water-based resistors. NASA MSFC has provided labor, materials and supplies, vacuum chambers over the last four years and most recently was critical to achieving operation of the control system, which became operational in December 2016. Boeing paid for the 15,000 gallons of transformer oil needed for the capacitor bank and the water deionization system needed for the transmission line. Y-12 has invested internal funds for several years to develop the technology needed to make 100 micron diameter wires out of lithium deuteride necessary for our experiments. UAH initially donated $55,000 for shipping the machine to Huntsville, and cost shared $150,000 to match another $150,000 from the Boeing Company to pay for the water and oil systems and design and procurement of hardware for the MITL.

UAH received a subcontract worth $45,000 in collaboration with the Navy Research Laboratory in an award from ARPA-E to explore the feasibility of using Charger 1 for their frozen fiber deuterium targets. Looking ahead, continued interest from NASA is anticipated as evidenced by the ongoing support and in the space propulsion 'area of interest' listed for three different centers.

Figure 11. Charger 1 Fusion Propulsion Laboratory.

Figure 12. Aerophysics Research Center, the building housing Charger 1.

G. Plasma and Combustion

This research area encompasses two different topics under Dr. Xu: plasma-assisted ignition and combustion (PAIC) and microplasma physics. PAIC is the use of electromagnetic field and ionized discharges to control or enhance the combustion process. The area can be divided into discharging or non-discharging systems. In discharging system, a very high strength electric field, typically pulsed, is initiated between two closely-spaced electrodes to produce a plasma discharge that generates ions, electrons, and neutral species such as O, H, OH, and other combustion radicals. Discharging systems are studied for combustion ignition at off-nominal conditions such as ultra-lean mixtures. Non-discharging systems have much lower electric fields that can be steady, pulsed, or AC. These systems utilized the ions and electrons produced naturally in hydrocarbon combustion via chemical ionization. As the name suggests, the non-discharging system does not produce a plasma discharge and instead applies electric forces on the existing ions and electrons. Non-discharging system are studied for flame stability.

Microplasma physics is a relatively new area in the last twenty years. These are plasma discharges generated at millimeter or smaller scales. The small size of the discharge allows high pressure operation. Microplasma have high electron temperature of 1-10 eV (1 eV = 11,600 K) but low ion and gas temperature of 300-500 K. Coupled with atmospheric-pressure or higher operation, these plasmas are of interest for surface coatings, biological treatments, and material synthesis.

In PAIC, UAH has the capability for both discharging and non-discharging systems. We have power sources capable of steady DC to 10 kHz pulsed DC. To-date, methane and propane have been tested with air or oxygen in PAIC experiments. The PRC also has the capability for liquid and solid fuels as well. The experimental equipment includes both simple atmospheric pressure burners as well as pressurized combustors. The diagnostics available for this research at the PRC include Langmuir probes, high-speed imaging, chemiluminescence, emissions spectroscopy, and laser induced fluorescence. In microplasmas, the same set of power sources and diagnostics can be applied to study atmospheric pressure discharges. We have two small vacuum chambers suitable for variable pressure testing with different gases down to 10^{-6} Torr as well as a large vacuum chamber for environmental testing.

Recent papers published in PAIC have demonstrated, for the first time, the suppression of thermoacoustic instabilities in a Rijke tube using solely electric fields.[69,70] Publications in microplasma have focused on diagnostic development to study these small scale plasmas using physical and optical technique.[71,72] A new project in microplasma for diode pumped rare gas lasers is beginning at the PRC supported by the Army Space Missile Defense Command.

H. Computational Modeling

Accurate modeling of radiative heat transfer is critical to atmospheric science applications, as well as propulsion systems, including combustion chambers and rocket-engine plumes. The objectives of our study are to: (1) predict radiative heat transfer using the wide band, narrow band, and global property models, and (2) compare the results obtained with those from line-by-line (LBL) simulations performed using the latest HITRAN and HITEMP databases. The five radiative property models considered in the current study are the Edwards Wide Band Model[73] (EWBM), Spectrally-Resolved Exponential Wide Band Model (SR-EWBM), Elsasser Narrow Band Model[74] (Elsasser NBM), Malkmus Narrow Band Model[75] (Malkmus NBM), and the Spectral Line Weighted-Sum-of-Gray-Gases[76] (SLW) model. The problem considered consists of a non-gray, one-dimensional (1-D) enclosure containing H_2O with uniform temperature and species mass fraction. The radiative transfer equation (RTE) was solved using the Discrete Ordinates Method (DOM). Figure 13 shows the results. First, the spectral absorption coefficients computed from these models are compared with the LBL data obtained using the HITRAN and HITEMP databases. The effects of varying the medium temperature and pressure, as well as the wall temperature, on the model predictions of radiative heat flux and its divergence are studied through comparison with the corresponding data obtained using HITRAN and HITEMP. For all of the medium temperatures and pressures considered, the SLW model predictions showed excellent agreement and Malkmus NBM showed reasonable agreement with the HITEMP data. At lower temperatures (and at constant pressure), the two wide band models and the Elsasser NBM showed reasonable agreement with HITEMP. At high temperatures (and at constant pressure), the SR-EWBM and the Elsasser NBM showed poor agreement with HITEMP. At low pressures (and at constant temperature), the two wide band models and the Elsasser NBM showed reasonable agreement with HITEMP. However, at high pressures, the EWBM showed poor agreement with HITEMP. Finally, we investigate DOM for a variety of cases, including isothermal, homogeneous, non-isothermal, inhomogeneous, and mixture cases for HITRAN and HITEMP. Two-dimensional domains, as well as spatial inhomogeneities in temperature and species concentrations, will also be considered in the future work.

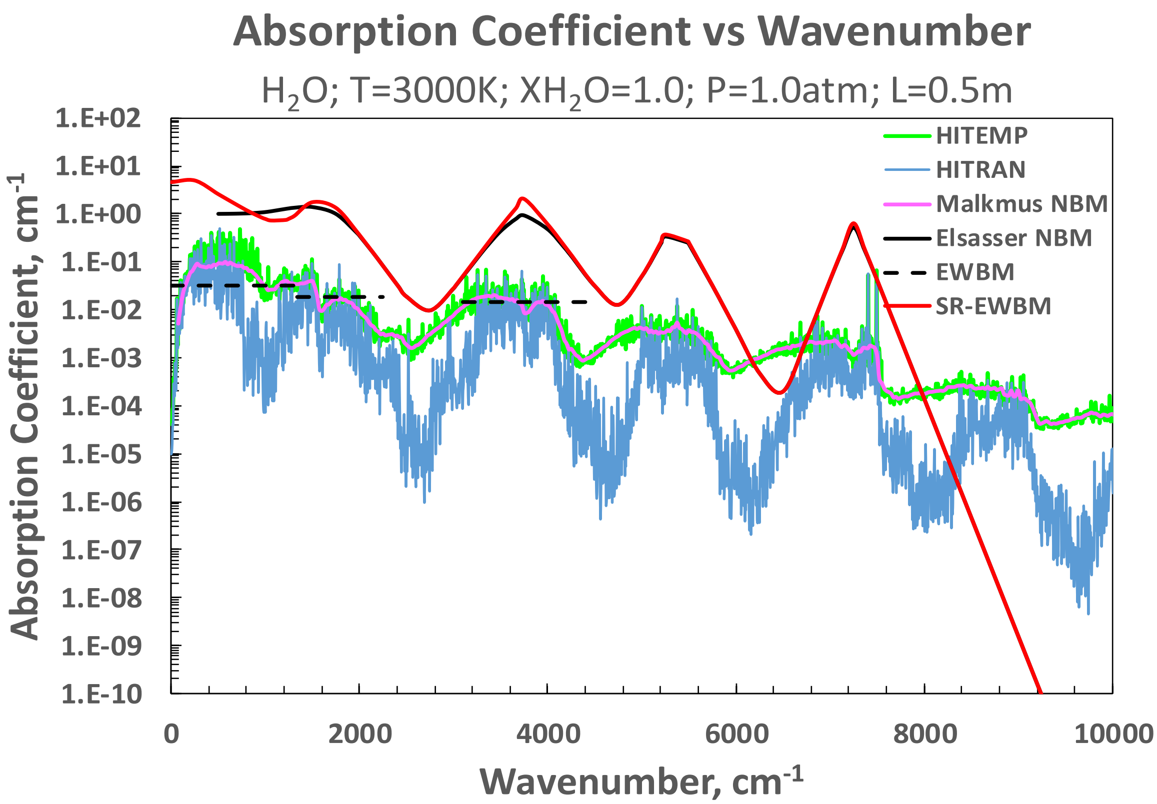

Figure 13. Absorption coefficient of H_2O at a pressure of 1.0 atm, temperature of 3000 K, and a mole fraction of 1.0 are shown as a function of wavenumber. Line-by-line absorption coefficients obtained from the HITEMP[77] 2010 and HITRAN[78] 2012 databases are compared with the absorption coefficients predicted using the Malkmus NBM, Elsasser NBM, EWBM, and SR-EWBM.

I. Aerospace Materials and Structures

The Aerospace Materials and Structures group at the PRC specializes in materials relevant to a diverse set of aerospace applications ranging from advanced alloys for structural application to novel materials for energy conversion and storage. The group is comprised of UAH Mechanical & Aerospace Engineering faculty and research staff from the UAH Research Institutes. Here, we highlight recent efforts in additive manufacturing led by Dr. Judy Schneider, 3D X-ray imaging of energy materials and propellants led by Dr. George Nelson, and material functionality under extreme environments led by Dr. Hazeli.

1. Use of Additive Manufacturing in Aerospace Materials and Structures

A major component of a liquid rocket engine (LRE) is the combustion chamber and nozzle. This contains the hot combustion gases as they are injected into the chamber, pass through the throat, and are expanded into the nozzle and skirt providing the thrust needed to propel the LRE upward.[79] Depending on the propellants, the combustion gases can exceed 3300º C, a very severe environment for material survivability. Thus, the design and fabrication of a large LRE assembly relies on a tradeoff between overall weight and survivability. While the lightest weight solution would be fabrication from monolithic materials that can withstand the combustion environment without various cooling schemes, these are generally expensive or have limited availability. Carbon/carbon nozzle construction provides the lightest weight option without cooling, but the materials are costly and facilities to construct large composite structures are limited, if they exist at all. Metals, such as rhenium, could survive the combustion environment without cooling, but their use is cost prohibitive.

To be able to fabricate the LRE assembly from less exotic metals and alloys, active internal coolant passages are used in the chamber and in the nozzle region just downstream of the throat. Typically, the alloy selection is based on the desired property of either strength (Ni based) or conductivity (Cu based). The incoming liquid propellants flow through the coolant passages to remove heat from the chamber, thereby preheating them in a regenerative fashion. Various fabrication options have been explored to produce the bi-metallic combustion chamber/nozzle components with internal coolant passages. Past design approaches have explored the use of brazed tube bundles, channel wall nozzles, slotted chamber/electroplated close-out jacket, and diffusion bonded platelet construction.[80] Many of these fabrication technologies were used in the construction of the Space Shuttle Main Engine (SSME) or RS-25.

While the RS-25 engine design flew for over 30 years, each LRE assembly was very costly with conservative estimates of $48 million each.[81] With the retirement of the Space Shuttle, the NASA and other companies are investigating various advanced design concepts and fabrication techniques for LRE combustion chamber/nozzles to be used on the Space Launch System (SLS) to reduce fabrication time and costs. The first stage of the SLS uses the RS-25 LREs which is driving the need to reduce production costs. Advanced materials and manufacturing technologies will be required to meet this challenge to reduce the weight and the fabrication time while producing a low cost component with high structural integrity.

One of the emerging new technologies being pursued for the fabrication of LRE components is the use of additive manufacturing (AM) processes which can result in a significant time savings and cost reduction. AM can be used to build complex shapes in low volumes on one platform. Use of powder bed AM is a viable solution for performance improvements and reduction of manufacturing time and cost of smaller complex, monolithic components such as injectors, valve housings, and turbine components. Other techniques being applied to the fabrication of larger combustion chambers/nozzles with multi-materials are referred to as free form or direct metal deposition and use either blown powder and wire feed. These techniques print “outside the box” and are not limited in size or to the use of monolithic feed stock. However most of the companies with the technology to produce AM parts lack the necessary resources to evaluate the resulting material property which is controlled by the processing parameters of heat source and deposition patterns. Control of the heat input and resulting microstructural development is very complex owing to the non-equilibrium conditions of localized rapid heating, solidification, and re-melting. Various modeling efforts are underway to understand and control the relationship between the process parameters and resulting temperature gradients during a build.

The NASA-MSFC has invested heavily in powder bed technologies for the smaller monolithic components. Complimentary research in Dr. Schneider’s laboratory at UAH is focused on evaluation of the various “out of the box” AM methods. Under various grants including NASA and Navy STTRs, she is engaged with several of the leading manufactures of free form or direct metal deposition printing.[82-84] Figure 14 a) shows a typical bi-metallic interface between copper and inconel alloys. This provides opportunities for her students to internship at various companies to assist in production of test specimens for characterization and testing at UAH. In parallel, her research group is also developing a continuum level, transient heat transfer model to capture the temperature distribution in an AM build.[85,86] Ultimately this will be integrated into a production setting to predict the temperature profile and guide selection of processing parameters and deposition strategy. For integration of temperature prediction, resulting microstructure and properties, a free form AM system, shown in Fig. 14 b), is being designed by a team of undergraduates for their senior capstone design project at UAH.

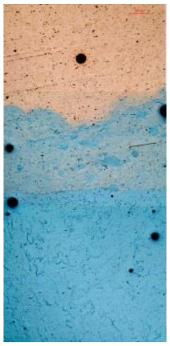

a) b)

Figure 14. a) Typical interface achieved in free form AM between copper and Inconel alloys. b) Overview of free from AM system being developed at UAH by undergraduate capstone design class.

2. 3D X-ray Imaging for Aerospace Materials and Structures

Next generation aerospace systems, from commercial aircraft to defense technology, present a growing need for onboard power, often in reduced volumes. The advanced power technologies that will support this expansion, particularly batteries and other electrochemical energy conversion and storage devices, require increased performance and reliability to ensure mission success. Multiscale functional materials form the cornerstone of these advanced technologies by storing energy, providing sites for chemical reactions and pathways for the transport of charge and chemical reactants. Direct observation of the structure of next generation energy storage and conversion materials can be achieved using non-destructive X-ray imaging methods.[87,88]

Using X-ray imaging methods PRC researchers led by Dr. George Nelson are actively exploring how the multiscale geometry of these systems influences coupled flows of mass, charge, and energy. This multiscale, multiphysics interaction has significant impacts on device performance and reliability. Most notably, this technique is being applied to the imaging and analysis of battery electrodes through two projects supported by the National Science Foundation. These projects focus on high capacity alloy anodes and spinel cathodes for lithium ion batteries. Alloy anodes offer significantly higher Li storage capacity compared to graphite anodes, but lithium storage in these materials generates substantial volume change (~180%) and accelerates performance degradation. Dr. Nelson's team has recently demonstrated the capability for spectroscopic imaging of these materials using a synchrotron X-ray source.[89] The observation of these changes during operation is being pursued. The effect of microstructural geometry on electrode performance is also being analyzed through experimental studies[90] and the use of nanotomography data as computational domains in finite element simulations.[91,92] The process of integrating microstructural data with computational modeling is illustrated in Fig. 15.

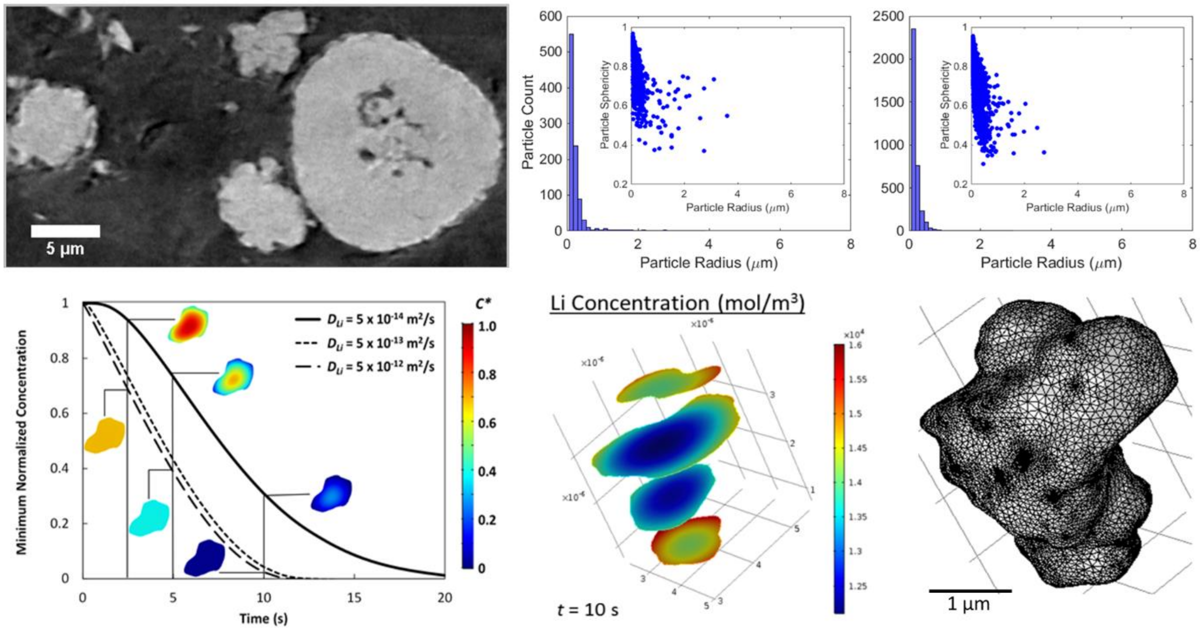

Figure 15. The analysis process for X-ray nanotomography data (clockwise from upper left) starts with a grayscale image of the electrode microstructure. Microstructural characterization provides particle geometric data. Meshing and subsequent computational modeling permits correlation of microstructure to performance.[91]

In addition to battery materials, Dr. Nelson's team is applying X-ray imaging methods to the study of porous hybrid rocket motors.[93,94] Using the PRC X-ray imaging facility, these studies have revealed the internal pore structure of end-burning porous hybrid grains, Fig. 16. As with the energy materials noted above, this complex pore structure supports oxidant flow to the grain's burn surface influencing the burn rate and thrust. The 3D image data permits non-destructive measurement of porosity, pore sizes, internal surface area, and pore connectivity. These characteristics are expected to provide insight into the influence porous grain microstructure on hybrid motor performance.

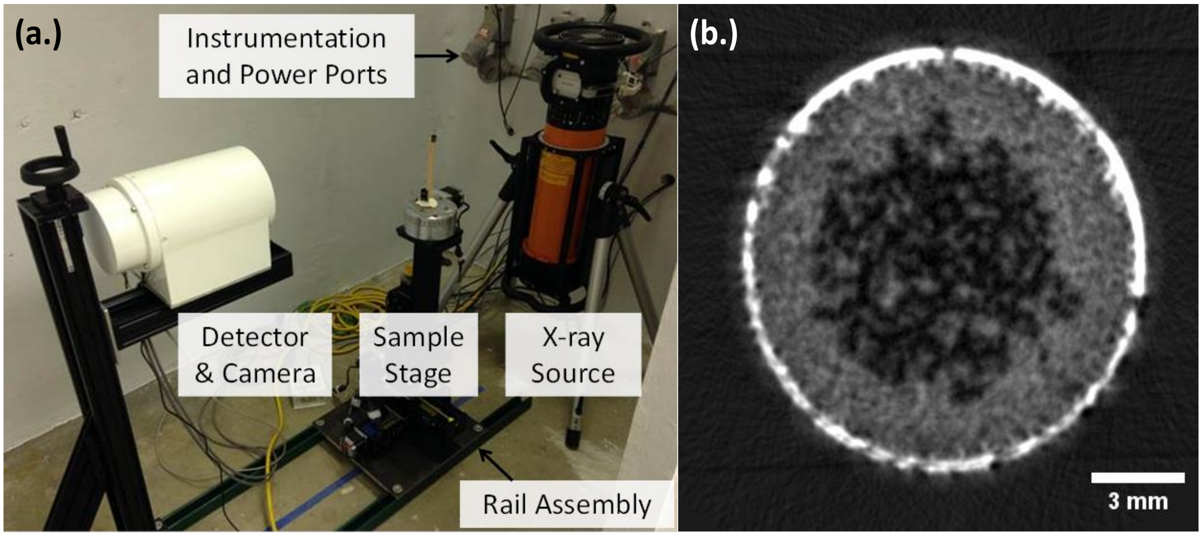

a) b)

Figure 16. a) The X-ray imaging system at the UAH Propulsion Research Center supports real time radiography of chemically active samples and 3D tomography of inactive samples. b) A tomographic cross-section of a porous hybrid rocket motor taken with this system reveals anisotropic porosity within the propellant grain.[93,94]

3. Microstructure Quantification under Extreme Environments

The main objective of Dr. Hazeli's group is to develop fundamental knowledge required to enhance material functionality under extreme environments such as high strain rate deformation, elevated temperatures, impact, high radiation fluxes, or a multitude of the above factors for defense, aerospace and propulsion applications. The goal is to investigate the constitutive response and roles of evolving intrinsic field variables to provide kinematic, kinetic, and dynamic descriptions of failure mechanisms in critical structural materials. Dr. Hazeli's current concern is on understanding instability and failure of lattice structures at different strain rates. Lattice structures combine mechanical properties of metals with various geometrical topologies, creating considerable potentials for light-weight energy-absorbent structures, thermal management, and supports for vehicle and spacecraft appendages.

His lab, shown in Fig. 17, has the capability of performing multi-scale materials characterization covering a wide range of strain rates and temperatures. Specifically, they can conduct low and high cycle fatigue, dynamic compression (up to $10^4 s^{-1}$), and tension (up to $10^3 s^{-1}$) experiments all in the range from ambient temperature to 1,000°C. In addition, they can study materials under hypervelocity impacts (up to $10^7 s^{-1}$) and radiation dominated plasma at the Aerophysics Research Center (ARC) in UAH.

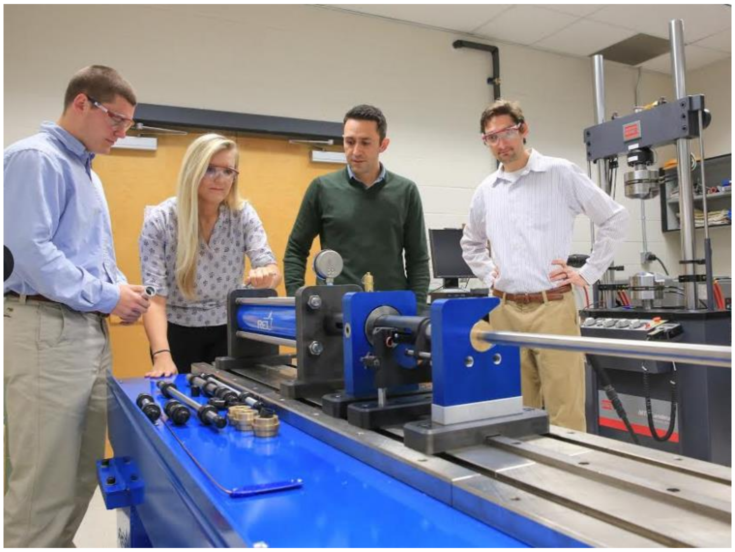

Figure 17. Performing high strain rate deformation test using split Hopkinson pressure bar (Kolsky bar). High strain rate data are required for safety and structural integrity assessment of structural materials subjected to impact and dynamic loading. Left to right: Andrew Minor (MS student), Madison Frederick (BS student), Dr. Hazeli, and Joe Indeck (PhD student)

J. Propellants and Energetics

1. Electrolytic Combustion Investigations

This research activity is under the direction of Dr. Robert Frederick and Dr. James Baird with support from Dr. David Lineberry and performed by Ph.D. students Andrew Hiatt and Joshua Lang. The work is sponsored by the Missile Defense Agency. The fundamental research involves experiments and analysis of electric solid propellants. These propellants ignite and extinguish under certain conditions upon the application and removal of electrical power applied to electrodes in contact with the propellant surface as illustrated in Fig. 18. For the propellant and conditions investigated, the experimental program revealed that combustion occurred at the anode or the cathode depending on the electrode area ratio configuration.[95] Furthermore, a fundamental electrolytic theory describing the possible chemistry and physics behind the observed phenomena at atmospheric conditions has been developed and presented.[96] The current theory accounts for the effects of polarity and electrode area ratio. Additional experiments and theoretical work continue.

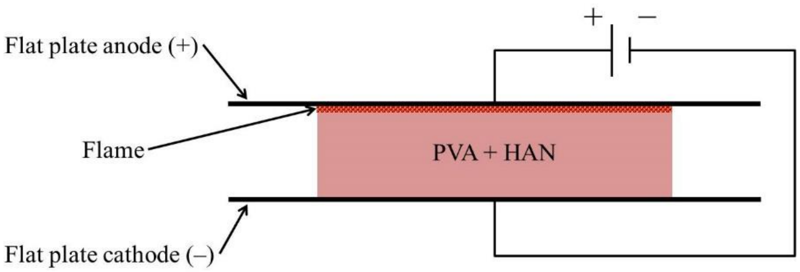

Figure 18. Representative chemical composition of an electric solid propellant consisting primarily of polyvinyl alcohol (PVA) and hydroxylammonium nitrate (HAN) and the electric circuit used for ignition.[95]

2. Injector Spray Investigations

This research activity was under the direction of Dr. Robert Frederick with support from Dr. David Lineberry. The work has been sponsored by Alabama Space Grant Fellowships, NASA MSFC, and internal UAH funding. Doctoral students Chad Eberhart[3]and Brian Sweeney[6] received Ph.D.'s last year as a result of their dissertations and publications on this work. The overall objective of the work is to understand the fluid dynamics of different rocket injector elements and the resulting spray behaviors though experimental investigations of water and air flows by controlling the injector dimensional and flow configurations.

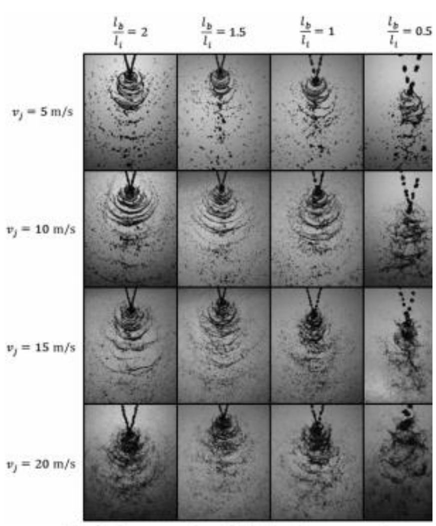

Figure 19. Spray Snapshots: 90 degree impingement angle.[97]

The impinging injector research examined the effect of jet breakup length on the spray characteristics of like doublet injectors[97] Cold-flow experiments using water at atmospheric pressure systematically determined the effect of the jet breakup length to impingement distance ratio on spray characteristics for like-doublet injectors as shown in Fig. 19. For ratios greater than one, a flat sheet was formed that subsequently disintegrated into waves of ligaments and droplets. The breakup length of the sheet increased with the Weber number up to a transition point where it began to decrease with further increases of the Weber number. For ratios equal to one, an unsteady flat sheet was formed due to the jets intermittently disintegrating before reaching the impingement point. New empirical sheet breakup length and transition correlations were developed for these configurations. For ratios less than one, no sheet was formed. In addition, measurements of the ligament wavelengths and centerline droplet diameters were conducted for jet breakup length to impingement distance ratios greater than or equal to one. The mean ligament wavelengths were nearly constant for all operating conditions, impingement angles, and ratios. However, larger impingement angles and jet velocities corresponded with smaller mean droplet diameters and reduced spray polydispersity. Mean droplet diameters were independent of the jet breakup length to impingement distance ratio.

Several experimental and analytical studies pertaining to different aspects of swirl injector dynamics were published last year as well.[98-100] In the experimental work, the lower boundaries at which an injector's spray switches from non-pulsatile behavior to self-pulsation were experimentally characterized under water and air flow conditions for a liquid-centered swirl coaxial element configured both with and without inner post recess as shown in Fig. 20. Data-based modal decomposition analyses were used to extract distinct near-field spray dynamics from high-speed Schlieren imagery. Liquid stripping from the contiguous spray cone was observed in a flow regime where coaxial flows are known to experience fiber-type breakup due to hydraulic and aerodynamic instabilities. These periodic, non-pulsatile spray breakup patterns were detected as a precursor to self-pulsation. The frequency of these non-pulsatile patterns ranged from ∼1–4 kHz and compared well with the frequency of self-pulsation at its onset, which directly supports conventional ideas related to the mechanism of self-pulsation. The transition of spray dynamics from non-pulsatile to self-sustained oscillations showed a destabilizing/stabilizing effect as gas velocity increases, establishes a temporally unstable spray oscillation at onset, and suggests that self-pulsation may be excited when stripping behavior engages one or more fluid oscillators of the injector element. Different fluid oscillators within the injector were assessed analytically and their contribution to the self-pulsation phenomenon were studied.[100]

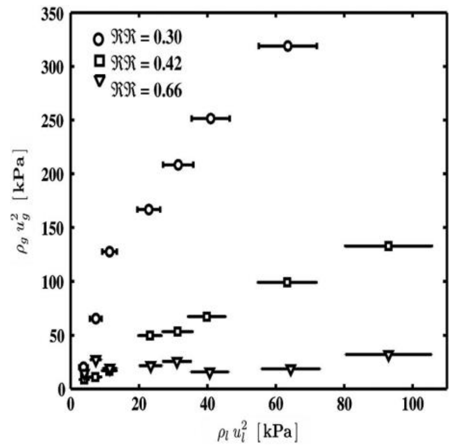

Figure 20. Lower boundaries of self-pulsation for each test recess ratio configuration of swirl-coaxial injector.[99]

3. Axial-Injection, End-Burning Hybrid Motor Investigations

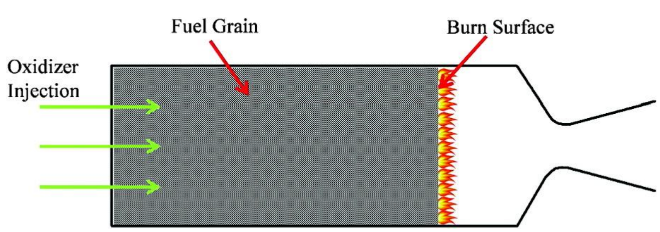

Figure 21. Axial-injection, end-burning hybrid.[103]

This research activity was under the direction of Dr. Robert Frederick with assistance from Dr. David Lineberry. Matthew Hitt conducted the study and received a Ph.D.[4] for a dissertation on this topic in 2016. The work was supported by a SMART Fellowship and internal UAH funding. The research evaluated the burning rate characteristics and process of axial-injection, end-burning hybrid rocket motors in order to increase the fuel regression rates.[101,102,] In this configuration, the oxidizer flows through a porous grain or small ports to the burning surface where combustion occurs. This design is in contrast to conventional hybrids where combustion occurs in ports cast into the grain. The configuration of an axial-injection, end-burning hybrid rocket motor is shown in Fig. 21.[103] Testing was conducted using polyethylene as the porous fuel and gaseous oxygen as the oxidizer. Nominal test articles were tested using 200, 100, 50, and 15 μm pore sizes. Propellants tested included polyethylene for the fuel and gaseous oxygen and nitrous oxide for the oxidizer. Experimental results confirmed that the regression rate of the porous axial-injection, end-burning hybrid was a function of the chamber pressure, as opposed to the oxidizer mass flux typical in conventional hybrids. Pressures tested ranged from atmospheric to 1194 kPa, yielding regression rates ranging from approximately 0.20 mm/s at atmospheric pressure to 8.89 mm/s at 1194 kPa. To describe the motor physics, an analytical model was developed based on a standard ablative model modified to include oxidizer flow through the grain. The heat transfer from the flame was primarily modeled using an empirically determined flame coefficient that included all heat transfer mechanisms in one term. In addition, an exploratory flame model based on the Granular Diffusion Flame model used for solid rocket motors was also adapted for comparison with the empirical flame coefficient. This model showed agreement with the experimental results, indicating that it has potential for giving insight into the flame structure in this motor configuration.

K. Propulsion Systems Technology Testbed

1. UAH Student Launch Initiative (SLI) Team

The UAH Charger Rocket Works competed in the NASA Student Launch Competition on April 8, 2017 in Bragg Farm Alabama. The team designed, built, and flew a sounding rocket to 5,160 feet in the national launch competition. The team consisted of 15 students from the UAH Mechanical & Aerospace Engineering department. The 6-in. diameter rocket was 119 in. long, and was launched on an Aerotech L2200 solid rocket motor. The rocket airframe had a secondary set of actively controlled fins located forward of the main to control the roll rate of the rocket. Throughout the 9 month program, the team conducted 2 subscale and 5 full scale flights to verify the aerodynamics of the rockets and the roll control system design. In the competition, the UAH team placed 4th nationally. The team designed and built the rocket as part of a senior design class in the Mechanical & Aerospace Engineering Department at UAH under the direction of Dr. David Lineberry and Mr. Jason Winningham.

Figure 22. UAH 2016-2017 SLI team and team mentor Jason Winningham pose with their rocket at the Student Launch National Competition.

2. Propulsion Testing

During the 2016-2017 academic year, the PRC conducted tests of solid rocket motors, hybrid engines, and liquid rocket engines for a variety of customers including Gloyer-Taylor Laboratories, NASA MSFC, Vector Space Systems, C3 Propulsion, and the Missile Defense Agency. Test campaigns included hot fire testing with liquid oxygen, nitrous oxide, RP-1, and methane propellants, AP composite solid rocket motors, and HTPB based hybrid motor grains. Testing included thrust levels up to 500 lb_f and chamber pressures up to 800 psi.

IV. People Make the Difference

During the past year, we continued to intentionally build relationships with each other and our community. The PRC hosted monthly student mentoring cookout lunches at the lab that included guest speakers and tours of the facilities for guests. We hosed our 25th anniversary celebration in October of 2016, which featured a banquet, a propulsion symposium with joint talks from alumni and current students, and a cookout at the lab. Over 200 people participated in these celebratory events. Our PRC Student Association (PRCSA) continued to support outreach events such as Girls Science and Engineering Day, the regional Science Olympiad, and NASA in the Park, a Huntsville tradition.

Each year we hold two celebrations honoring our upcoming graduates and all the departments around campus that provide the support that makes our efforts successful. Figure 23 shows the PRC team at our December 2016 gathering.

Figure 23. Propulsion Research Center faculty, staff, students, colleagues, and friends at the fall 2016 Recognition of Graduates Reception.

"*Keep relationships more important than tasks or problems*" –Dr. Robert A. Frederick, Jr.

V. Strategies for the Future

Current growth areas that we are pursuing include upgrading our Propulsion Test Capability for MDA Systems, adding run time capacity to our Supersonic Wind Tunnel, growing propulsion systems engineering research (starting with nuclear thermal propulsion systems), and the growth of additive manufacturing research for propulsion applications. The PRC will be completing a strategic planning exercise led by Dr. Dale Thomas this year.

Acknowledgments

The authors acknowledge the inputs and contributions of the faculty, staff, students, and graduates of the Propulsion Research Center for providing valuable inputs and suggestions for this paper. Molly Kitts, PRC Office Assistant, was the key contributor to compiling and editing this paper.

The support of the UAH Vice President for Research Office, and the UAH College of Engineering are gratefully acknowledged. Thanks also go to our recent sponsors: The Missile Defense Agency, The State of Alabama Department of Commerce, NASA MSFC, Hyper V Technologies, Boeing, Inc., Exquadrum, Inc., Varian Medical Systems, C3 Propulsion, Combustion Research and Flow Tech. Inc., Aerojet Rocketdyne, Analysis and Applications Inc., Department of the Navy – NRL, Gloyer-Taylor Laboratories, IHI Corporation, Jacobs, the State of Alabama, NASA Alabama Space Grant, Manufacturing Technology Solutions, and Solar Turbines. Grateful acknowledgement to all those potential customers who partnered with us to write proposals last year.

References

[1] Hawk, C.W. and Frederick, R.A., "University Propulsion Programs at the University of Alabama in Huntsville," AIAA Paper 2004-3323, July 2004.

[2] Frederick, R. A., "UAH Propulsion Research Center - 25th Anniversary Highlights," AIAA Paper 2016-4722, 2016, http://dx.doi.org/10.2514/6.2016-4722.

[3] Eberhart, C., "An Investigation of Liquid Rocket Swirl Coaxial Injection under Self-excited High Frequency Oscillations," Ph.D. Dissertation, Mechanical & Aerospace Dept., the Univ. of Alabama in Huntsville, Advisor: Dr. Robert Frederick, Jr., 2016.

[4] Hitt, M., "Regression Rate Study of Porous Axial-Injection, End Burning Hybrid Fuel Grains," Ph.D. Dissertation, Mechanical & Aerospace Dept., The Univ. of Alabama in Huntsville, Advisor: Dr. Robert Frederick, Jr., 2016.

[5] Dahriwal, R., "Stochastic Theory and Direct Numerical Simulations of the Relative Motion of High-Stokes-Number Particles in Isotropic Turbulence," Ph.D. Dissertation, Mechanical & Aerospace Dept., the Univ. of Alabama in Huntsville, Advisor: Dr. Sarma Rani, 2016.

[6] Sweeney, B., "Like-Double Injectors: The Effects of Varying the Impingement Distance and an Analysis of the Primary Atomization Zone," Ph.D. Dissertation, Mechanical & Aerospace Dept., The University of Alabama in Huntsville, Advisor: Dr. Robert Frederick, Jr., 2016.

[7] Jeffires, S., and Hirshorn, S., "Study on NASA's Technology Readiness Assessment (TRA) Process," presented at the NASA Program and Project Management Board, July 2014.

[8] Szajnfarber, Z. and Weigel, A. L., "A Process Model of Technology Innovation in Governmental Agencies: Insights from NASA's Science Directorate," *Acta Astronaut.*, vol. 84, pp. 56–68, Mar. 2013.

[9] "NASA Technology Roadmaps TA 11: Modeling, Simulation, Information Technology, and Processing," National Aeronautics and Space Administration, July 2015.

[10] Aueron, A., and Thomas, L. D., "Nuclear Thermal Propulsion System Modeling using Model Based Systems Engineering," *Joint Army Navy NASA Airforce (JANNAF) In-Space Chemical Propulsion Technical Interchange Meeting*, April 2017.

[11] Grilli, M., Schmid, P. J., Hickel, S., and Adams, N. A., "Analysis of Unsteady Behavior in Shockwave Turbulent Boundary Level Interaction," *Journal of Fluid Mechanics*, Vol. 700, pp. 16–28, 2012.

[12] Pirozzoli, S., Larsson, J., Nichols, J. W., Bernardini, M., Morgan, B. E., and Lele, S. K. "Analysis of Unsteady Effects in Shock/Boundary Layer Interactions," *Proceedings of the Summer Program 2010*, Center for Turbulence Research, pp. 153–164, 2010.

[13] Zhang, Q., O'Dowd, D. O., He, L., Wheeler, A. P. S., Ligrani, P. M., and Cheong, B. C. Y., "Overtip Shock Wave Structure and Its Impact on Turbine Blade Tip Heat Transfer, " *ASME Transactions-Journal of Turbomachinery*, Vol. 133, No. 4, pp. 041001-1 to 041001-8, 2011.

[14] Zhang, Q., O'Dowd, D. O., He, L., Oldfield, M. L. G., and Ligrani, P. M., "Transonic Turbine Blade Tip Aerothermal Performance with Different Tip Gaps—Part 1: Tip Heat Transfer," *ASME Transactions-Journal of Turbomachinery*, Vol. 133, No. 4, pp. 041027-1 to 041027-9, 2011b.

[15] Abhari, R. S., Guenette, G. R., Epstein, A. H., and Giles, M. B. "Comparison of Time-Resolved Turbine Rotor Blade Heat Transfer Measurements and Numerical Calculations," *ASME Transactions-Journal of Turbomachinery*, Vol. 114, No. 4, pp. 818-827, 1992.

[16] Hayashi, M., Aso, S., and Tan, A. "Fluctuation of Heat Transfer in Shock Wave/Turbulent Boundary-Layer Interaction," *AIAA Journal*, Vol. 27, No. 4, pp. 399-404, 1989.

[17] Lee, Y., Settles, G., and Horstman, C. "Heat Transfer Measurements and CFD Comparison of Swept Shock Wave/Boundary-Layer Interactions," *AIAA 28th Joint Propulsion Conference and Exhibit*, Paper No. AIAA-92-3665, Nashville, Tennessee, 1992.

[18] Nix, A. C., Diller, T. E., Ng, W. F., and Schetz, J. A., "Experimental Evaluation of Heat Transfer Effects of Shock Waves on Transonic Turbine Blades," *ASME International Mechanical Engineering Congress and Exhibition*, ASME Paper No. 97-WA/HT-1, Dallas, Texas, 1997.

[19] Schülein, E., "Skin Friction and Heat Flux Measurements in Shock/Boundary Layer Interaction Flows," *AIAA Journal*, Vol. 44, No. 8, pp. 1732-1741, 2006.

[20] Ligrani, P. M., Jiang, H., Lund, B., and Jin, J. S., "Deviations Due To Non-Newtonian Influences Within a Miniature Viscous Disk Pump," *ASME Transactions-Journal of Fluids Engineering*, Vol. 135, No. 3, Mar. 13, pp. 031205-1 to 031205-12.

[21] Blanchard, D. B., Ligrani, P. M., and Gale, B. K., "Miniature Single-Disk Viscous Pump (Single-DVP), Performance Characterization," *ASME Transactions-Journal of Fluids Engineering*, Vol. 128, No. 3, May 2006, pp. 602-610.

[22] Lund, B., Ligrani, P. M., and Fatemi, A., "Onset and Transition to Elastic Turbulence: Effects of Rheological Property Variations for Polyacrylamide-Water Solutions," *20th International Colloquium Tribology – Industrial and Automotive Lubrication*, Stuttgart/Ostfildern, Germany, Jan. 2016.

[23] Lund, B., Ligrani, P. M., and Brown, M., "Development and Control of Elastic Turbulence within a Micro-Scale Viscous Disk Pump," *Advances and Applications in Fluid Mechanics* Journal, Vo. 19, No. 3, Aug. 2016, pp. 517-539.

[24] Ligrani, P. M., Lund, B., and Fatemi, A., "Miniature Viscous Disk Pump: Performance Variations From Non-Newtonian Elastic Turbulence," *ASME Transactions-Journal of Fluids Engineering*, Vol. 139, No. 2, Feb. 2017, pp. 021104-01 to 021104-10.

[25] McKinley, G. H., Pakdel, P., Oztekin, A., "Rheological and Geometric Scaling of Purely Elastic Flow Instabilities," *Journal of Non-Newtonian Fluid Mechanics*, Vol. 67, 1996, pp. 19-47.

[26] James, D. F., "Boger Fluids," *Annual Review of Fluid Mechanics*, Vol. 41, 2009, pp. 129-142.

[27] Abed, W. M., Whalley, R. D., Dennis, D. J. C., and Poole, R. J, "Experimental Investigation of the Impact of Elastic Turbulence on Heat Transfer in a Serpentine Channel," *Journal of Non-Newtonian Fluid Mechanics*, Vol. 231, 2016, pp. 68-78.

[28] Whalley, R. D., Abed, W. M., Dennis, D. J. C., and Poole, R. J, "Enhancing Heat Transfer at the Micro-Scale Using Elastic Turbulence," *Theoretical and Applied Mechanics Letters*, Vol. 5, 2015, pp. 103-106.

[29] Traore, B., Castelain, C., and Burghelea, T, "Efficient Heat Transfer in a Regime of Elastic Turbulence," *Journal of Non-Newtonian Fluid Mechanics*, Vol. 223, 2015, pp. 62-76.

[30] De Gennes, P. G., "Coil-Stretch Transition of Dilute Flexible Polymers under Ultrahigh Velocity Gradients," *Journal of Chemical Physics*, Vol. 60, No. 12, 1974, pp. 5030 to 5042.

[31] Naschie, M. S. E., Athel, S. A., and Kapitaniak, T., “A Note on Elastic Turbulence and Diffusion,” *Journal of Sound and Vibration*, Vol. 155, No. 3, 1992, pp. 515-522.

[32] Burghelea, T., Segre, E., and Steinberg, V., “Elastic Turbulence in Von Karman Swirling Flow Between Two Disks,” *Physics of Fluids*, Vol. 19, 2007, pp. 053104-1 to 053104-26.

[33] Ligrani, P. M., Copeland, D., Ren, C., Su, M., and Suzuki, M., “Heat Transfer Enhancements From Elastic Turbulence Using Sucrose-Based Polymer Solutions,” *AIAA Journal of Thermophysics and Heat Transfer*, to appear 2017.

[34] Copeland, D., Ren, C., Su, M., and Ligrani, P. M., “Elastic Turbulence Influences and Convective Heat Transfer within a Miniature Viscous Disk Pump,” *International Journal of Heat and Mass Transfer,* to appear 2017.

[35] Rogers, N., Ren, Z., Buzzard, W. C., Sweeney, B., Tinker, N., Ligrani, P. M., Hollingsworth, K. D., Liberatore, F., Patel, R., Ho, S., and Moon, H. K., “Effects of Double Wall Cooling Configuration and Conditions on Performance of Full-Coverage Effusion Cooling,” *ASME Transactions-Journal of Turbomachinery*, Vol. 139, No. 5, May 2017, pp. 051009-01 to 051009-13.

[36] Ren, Z., Vanga, S. R., Rogers, N., Ligrani, P. M., Hollingsworth, K. D., Liberatore, F., Patel, R., Srinivasan, R., and Ho, Y., “Internal and External Cooling of a Full Coverage Effusion Cooling Plate: Effects of Double Wall Cooling Configuration and Conditions,” Paper Number GT2017-64921, *ASME TURBO EXPO 2017: Turbomachinery Technical Conference and Exposition*, Charlotte, North Carolina, June 2017.

[37] Ligrani, P. M., Ren, Z., Liberatore, R., Patel, R., Srinivasan, R., and Ho, Y., “Double Wall Cooling of a Full Coverage Effusion Plate, Including Internal Impingement Array Cooling,” Paper Number IMECE2017-72066, *IMECE 2017*, *ASME International Mechanical Engineering Congress and Exposition*, Tampa, Florida, Nov. 2017.

[38] Buzzard, W. C., Ren, Z., Ligrani, P. M., Nakamata, C., and Ueguchi, S., “Influences of Target Surface Roughness on Impingement Jet Array Heat Transfer, Part 1: Effects of Roughness Pattern, Roughness Height, and Reynolds Number,” Paper Number GT2016-56354, *ASME TURBO EXPO 2016: Turbomachinery Technical Conference and Exposition,* Seoul, South Korea, June 2016.

[39] Buzzard, W. C., Ren, Z., Ligrani, P. M., Nakamata, C., and Ueguchi, S., "Influences of Target Surface Small-Scale Rectangle Roughness on Impingement Jet Array Heat Transfer," *International Journal of Heat and Mass Transfer*, to appear 2017.

[40] Buzzard, W. C., Ren, Z., Ligrani, P. M., Nakamata, C., and Ueguchi, S., "Influences of Target Surface Roughness on Impingement Jet Array Heat Transfer, Part 2: Effects of Roughness Shape, and Reynolds Number," Paper Number GT2016-56355, *ASME TURBO EXPO 2016: Turbomachinery Technical Conference and Exposition*, Seoul, South Korea, June 2016.

[41] Ren, Z., Buzzard, W. C., Ligrani, P. M., Nakamata, C., and Ueguchi, S., "Impingement Jet Array Heat Transfer: Target Surface Roughness Shape, Reynolds Number Effects," *AIAA Journal of Thermophysics and Heat Transfer*, to appear 2017.

[42] Ren, Z., Buzzard, W. C., and Ligrani, P. M., "Influences of Target Surface Cylindrical Roughness on Impingement Jet Array Heat Transfer: Effects of Roughness Height, Roughness Shape, and Reynolds Number," Paper Number IMECE2016-67655, *IMECE 2016: ASME International Mechanical Engineering Congress and Exposition*, Phoenix, Arizona, Nov. 2016.

[43] Ligrani, P. M., Ren, Z., and Buzzard, W. C., "Impingement Jet Array Heat Transfer with Small-Scale Cylinder Target Surface Roughness Arrays," *International Journal of Heat and Mass Transfer*, to appear 2017.

[44] Yang, L., Ren, J., Jiang, H., and Ligrani, P. M., "Experimental and Numerical Investigation of Unsteady Impingement Cooling Within a Blade Leading Edge Passage," *International Journal of Heat and Mass Transfer*, Vol. 71, Apr. 2014, pp. 57-68.

[45] Yang, L., Ligrani, P. M., Ren, J., and Jiang, H., "Unsteady Structure and Development of a Row of Impingement Jets, Including Kelvin-Helmholtz Vortex Development," *ASME Transactions-Journal of Fluids Engineering*, Vol. 137, No. 5, May 2015, pp. 051201-1 to 051201-12.

[46] Yang, L., Li, Y., Ligrani, P. M., Ren, J., and Jiang, H., “Unsteady Heat Transfer and Flow Structure of a Row of Laminar Impingement Jets, Including Vortex Development,” *International Journal of Heat and Mass Transfer*, Vol. 88, Sept. 2015, pp. 149-164.

[47] Li, W., Ren, J., Jiang, H., Luan, Y., and Ligrani, P. M, “Assessment of Six Turbulence Models For Modelling and Predicting Narrow Passage Flows, Part 1: Impingement Jets,” *Numerical Heat Transfer, Part A: Applications*, Vol. 69, No. 2, Jan. 2016, pp. 109-127.

[48] Li, W., Ren, J., Jiang, H., Luan, Y., and Ligrani, P. M, “Assessment of Six Turbulence Models For Modelling and Predicting Narrow Passage Flows, Part 2: Pin Fin Arrays,” *Numerical Heat Transfer, Part A: Applications*, Vol. 69, No. 5, Mar. 2016, pp. 445-463.

[49] Li, W., Li, X., Yang, L., Ren, R., Jiang, H., and Ligrani, P. M., “Effect of Reynolds Number, Hole Patterns, and Hole Inclination on Cooling Performance of an Impinging Jet Array - Part 1: Convective Heat Transfer Results and Optimization,” *ASME Transactions-Journal of Turbomachinery*, Vol. 139, No. 4, Apr. 2017, pp. 041002-01 to 041002-11.

[50] Winkler, S., Kerber, E., Hitz, T., Weigand, B., and Ligrani, P. M., “Numerical Second Law Analysis around a Turbine Guide Vane Using a Two-Equation Turbulence Model and Comparison With Experiments*,” International Journal of Thermal Sciences*, to appear 2017.

[51] Ligrani, P. M., and Jin, J. S., “Second Law Analysis of Aerodynamic Losses: Results for a Cambered Vane With and Without Film Cooling,” *ASME Transactions-Journal of Turbomachinery*, Vol. 135, No. 4, July 2013, pp. 041013-1 to 041013-14.

[52] Chung, Y. S., Lee, D. H., and Ligrani, P. M., “Jet Impingement Cooling of Chips Equipped With Cylindrical Pedestal Profile Fins,” *ASME Transactions-Journal of Electronic Packaging*, Vol. 127, No. 2, June 2005, pp. 106-112.

[53] Lee, D. H., Chung, Y. S., and Ligrani, P. M., “Jet Impingement Cooling of Chips Equipped With Multiple Cylindrical Pedestal Fins,” *ASME Transactions-Journal of Electronic Packaging*, Vol. 129, No. 3, Sept. 2007, pp. 221-228.

[54] Lee, D. H., Bae, J. R., Parks, H. J., Lee, J. S., and Ligrani, P. M., “Confined, Milliscale Unsteady Laminar Impinging Slot Jets and Surface Nusselt Numbers,” *International Journal of Heat and Mass Transfer*, Vol. 54, Nos. 11-12, May 2011, pp. 2408-2418.

[55] Lee, D. H., Park, H. J., and Ligrani, P. M., “Milliscale Confined Impinging Slot Jets: Laminar Heat Transfer Characteristics for an Isothermal Flat Plate,” *International Journal of Heat and Mass Transfer*, Vol. 55, Nos. 9-10, Apr. 2012, pp. 2249-2260.

[56] Lee, D. H., Bae, R. J., Ryu, M., and Ligrani, P. M., “Confined, Milliscale Unsteady Laminar Impinging Slot Jets: Effects of Slot Width on Surface Stagnation Point Nusselt Numbers,” *ASME Transactions – Journal of Electronic Packaging*, Vol. 134, No. 4, Dec. 2012, pp. 041004-1 to 041004-11.

[57] Kim, S. J., Kim, Y. H., Park, H. J., Lee, D. H., and Ligrani, P. M., “Heat Transfer Measurements From Concave and Convex Surfaces With a Fully Developed Confined Impinging Slot Jet,” *The 15th International Heat Transfer Conference*, IHTC2014, Kyoto, Japan, Aug. 2014.

[58] Lee, D. H., Park, H. J., and Ligrani, P. M., “Visualization and Structure of Confined, Milliscale, Unsteady Impinging Slot Jets and Associated Vortices,” *Experiments in Fluids*, Vol. 54:1420, 2013, pp. 1-15.

[59] Nivedita, N., Ligrani, P. M., and Papautsky, I., “Spiral Inertial Microfluidic Devices For Continuous Blood Cell Separation,” *MOEMS-MEMS Conference on Micro- and Nano-Fabricated Electromechanical and Optical Components*, Paper Number 8251-26, SPIE – International Society for Optics and Photonics, San Francico, Jan. 2012.

[60] Jennerjohn, M., Nivedita, N., Carlson, L., Ligrani, P. M., Papautsky, I., Eslick, J., Sprague, R., and Bowles, E., “Microfluidic Inertial, Continuous SPLITT, and Field-Flow Fractionation Developments for Separation of Whole Blood Components,” *16th International Symposium on Field- and Flow-Based Separations*, FFF2013-PAU, IPREM and Faculty of Sciences Pau, University de Pau et des Pays de l’Adour, France, June-July 2013.

[61] Ligrani, P. M., and Niver, R. D., “Flow Visualization of Dean Vortices in a Curved Channel with 40 to 1 Aspect Ratio,” *Physics of Fluids*, Vol. 31, No. 12, Dec. 1988, pp. 3605-3617.

[62] Ligrani, P. M., and Hedlund, C. R., “Experimental Surface Heat Transfer and Flow Structure in a Curved Channel with Laminar, Transitional, and Turbulent Flows,” *ASME Transactions-Journal of Turbomachinery*, Vol. 126, No. 3, July 2004, pp. 414-423.

[63] Nivedita, N., Ligrani, P. M., and Papautsky, I., “Dean Flow Dynamics in Low-Aspect Ratio Spiral Microchannels,” *Scientific Reports*, to appear, 2017.

[64] Nivedita, N., Ligrani, P. M., and Papautsky, I., “Evolution of Secondary Dean Vortices in Spiral Microchannels for Cell Separations,” *Miniaturized Systems for Chemistry and Life Sciences MicroTAS 2013*, University of Freiburg, Freiburg, Germany, October 2013.

[65] Adams, R. B., Cassibry, J. T., and Schillo, K., “Developing the Pulsed Fission-Fusion (PuFF) Engine,” *50th AIAA/ASME/SAE/ASEE Joint Propulsion Conference*. American Institute of Aeronautics and Astronautics, http://arc.aiaa.org/doi/abs/10.2514/6.2014-3520, 2015.

[66] Cassibry, J., Cortez, R., Stanic, M., Watts, A., Seidler, W., Adams, R., Statham, G., and Fabisinski, L., “Case and Development Path for Fusion Propulsion,” *Journal of Spacecraft and Rockets*, Vol. 52, No. 2, doi:10.2514/1.A32782, 2015, pp. 595–612.

[67] Ryutov, D. D., M. S. Derzon, and Matzen, M. K., “The Physics of Fast Z Pinches,” *Reviews of Modern Physics*, Vol. 72, No. 167, doi:10.1103/RevModPhys, 2000.

[68] Haines, M. G., “A Review of the Dense Z-Pinch,” *Plasma Physics and Controlled Fusion*, Vol. 53, No. 9, 093001, doi:10.1088/0741-3335/53/9/093001, 2011.

[69] Bradley, H., and Xu, K. G., “Electric Field Damping of Rijke Tube Combustion Instabilities,” *AIAA Journal of Propulsion and Power*, accepted, 2017.

[70] Salvador, P. R., and Xu, K. G., “Electric Field Modified Bunsen Flame with Variable Anode Placement,” *J. Thermophys. Heat Transf.*, accepted, 2017.

[71] Doyle, S. J., and Xu, K. G., “Use of Thermocouples and Argon Line Broadening for Gas Temperature Measurement in a Radio Frequency Atmospheric Microplasma Jet,” *Rev. Sci. Instrum.*, Vol. 88, No. 2, 2017.

[72] Xu, K. G., and Doyle, S. J., “Measurement of Atmospheric Pressure Microplasma Jet with Langmuir Probes Measurement of Atmospheric Pressure Microplasma Jet with Langmuir Probes,” *J. Vac. Sci. Technol*, Vol. 34, No. 5, 2016

[73] Edwards, D.K., and Menard, W.A., “Comparison of Models for Correlation of Total Band Absorption,” *Applied Optics*, Vol. 3, 1964, pp. 621-625.

[74] Elsasser, W.M., *Heat Transfer by Infrared Radiation in the Atmosphere*, Harvard UP, Cambridge, Massachusetts, 1943.

[75] Malkmus, W., "Random Lorentz Band Model with Exponential-Tailed S^{-1} Line-Intensity Distribution Function," *Journal of the Optical Society of America*, Vol. 57, No. 3, 1957, pp. 323-329.

[76] Denison, M.K., and Webb, B.W., "A Spectral Line-Based Weighted-Sum-of-Gray-Gases Model for Arbitrary RTE Solvers," *ASME Journal of Heat Transfer*, Vol. 115, 1993, pp. 1004-1012.

[77] Rothman, L. S., et. al. "The HITRAN2012 molecular spectroscopic database," *Journal of Quantitative Spectroscopy & Radiative Transfer*, Vol. 130, 2013, pp. 4-50.

[78] Rothman, L.S., et. al., "HITEMP, the high-temperature molecular spectroscopic database," *Journal of Quantitative Spectroscopy & Radiative Transfer*, Vol. 111, 2010, pp. 2139-2150.

[79] Sutton, G.P., *Rocket Propulsion Elements: an Introduction to the Engineering of Rockets*, 5th ed. pub., John Wiley & Sons, 1986.

[80] Gradl, P., Brandsmeier, W., Alberts, D., Walker, B., and Schneider, J., "Manufacturing Process Developments for Large Scale Regeneratively-cooled Channel Wall Rocket Nozzles," *JANNAF Programmatic and Industrial Base (PIB) / 11th Modeling and Simulation (MSS) / 9th Liquid Propulsion (LPS) / 8th Spacecraft Propulsion Joint Subcommittee Meeting*, Phoenix, AZ, Dec. 2016.

[81] Associated Press: National Edition, "Deep Discount on Space Shuttles," January 2010, pg. A20.

[82] Cordner, S., Prater, T., and Schneider, J.A., "Density Based Screening of Additively Manufactured Parts," *JANNAF TIM*, Huntsville, AL, Aug. 2016.

[83] Hill, T.C., Schneider, J.A., and Sporie, S., "Blown Powder Laser Deposition Study," *JANNAF TIM*, Huntsville, AL, Aug. 2016.

[84] Schneider, J.A., Hyatt, G., and Babai, M., "Blown Powder Laser Deposition Additive/Subtractive Processing," *AMMO DOD presentation*, Aug. 2016.

[85] Stockman, T., and Schneider, J. A., "Full Build Thermal Modeling of the Additive Manufacturing Process," *Young Professional AIAA Conference*, Huntsville, AL, Oct. 2016.

[86] Stockman, T., Schneider, J.A., and Walker, B., "Managing Thermal History in Free Form Additive Manufacturing," *JANNAF TIM*, Huntsville, AL, Aug. 2016.

[87] Nelson, G. J., van Zandt, Z. K., and Jibhakate, P. D., "Direct X-ray Imaging as a Tool for Understanding Multiphysics Phenomena in Energy Storage," *ASME Journal of Electrochemical Energy Conversion and Storage*, Vol. 13, No. 3, 2016, Article 030802.

[88] Cocco, A. P., Nelson, G. J., Harris, W. M., Nakajo, A., Lombardo, J. J., Myles, T. D., Kiss, A. M., and Chiu, W. K. S., "Three Dimensional Microstructural Imaging Methods for Energy Materials," *Physical Chemistry Chemical Physics*, Vol. 15, No. 39, 2013, pp. 16377-16407.

[89] L. J. Ausderau, H. J. Gonzalez, J. R. Buckley, V. De Andrade, Y. Liu and G. J. Nelson, "Elemental and Chemical Mapping of High Capacity Intermetallic Li-ion Anodes with Transmission X-ray Microscopy," *JOM*, 2017, in press.

[90] Jibhakate, P. D., and Nelson, G. J., "Fabrication and Characterization of Nanostructured Cathodes for Li-Ion Batteries," *Proceedings of IMECE2016: 2016 ASME International Mechanical Engineering Congress and Exposition*, Phoenix, Arizona, Nov. 2016.

[91] Nelson, G. J., Ausderau, L. J., Shin, S. Y., Buckley, J. R., Mistry, A., Mukherjee, P. P., and De Andrade, V., "Transport-Geometry Interactions in Li-ion Cathode Materials Imaged Using X-ray Nanotomography," *Journal of the Electrochemical Society*, 2017, Vol. 164, No. 7, A1412-A1424.

[92] Nelson, G. J., "A Numerical Investigation of Active Surface Accessibility in Li-ion Battery Cathodes," *Proceedings of IMECE2016: 2016 ASME International Mechanical Engineering Congress and Exposition*, Phoenix, Arizona, Nov. 2016.

[93] Buckley, J. R., Denny, M. D., and Nelson, G. J., "Computed Tomography Characterization of a Porous Hybrid Motor Grain," *51st AIAA/SAE/ASEE Joint Propulsion Conference*, Orlando, Florida, July 2015.

[94] Buckley, J. R. and Nelson, G. J., "Computed Tomography Characterization of a Porous Hybrid Motor Grain with added Contrast Agent," *52nd AIAA/SAE/ASEE Joint Propulsion Conference*, Salt Lake City, Utah, July 2016.

[95] Hiatt, A. T., and Frederick, R. A., "Laboratory Experimentation and Basic Research Investigating Electric Solid Propellant Electrolytic Characteristics," AIAA Paper 2016-4935, July 2016, http://dx.doi.org/10.2514/6.2016-4935.

[96] Baird, J. K., Lang, J. R., Hiatt, A. T., and Frederick, R. A., "Electrolytic Combustion in the Polyvinyl Alcohol + Hydroxylammonium Nitrate Solid Propellant," AIAA Paper 2016-4908, July 2016, http://dx.doi.org/10.2514/6.2016-4908.

[97] Sweeney, B., and Frederick, R. A., "Jet Breakup Length to Impingement Distance Ratio for Like-Doublets," *AIAA Journal of Propulsion and Power*, Vol. 32, No. 6, 2016, pp. 1516-1530.

[98] Eberhart, C. J., and Frederick, R. A., "Fluid Oscillations of a Swirl Coaxial Injector under High-Frequency Self-Pulsation," *AIAA Journal of Propulsion and Power*, advance, https://doi.org/10.2514/1.B36177.

[99] Eberhart, C. J., and Frederick, R. A., "Details on the Mechanism of High-Frequency Swirl Coaxial Self-Pulsation," *AIAA Journal of Propulsion and Power*, advance, https://doi.org/10.2514/1.B36216.

[100] Eberhart, C. J., and Frederick, R. A., "Parametric Evaluation of Swirl Injector Dynamics in the High-Frequency Range," *AIAA Journal of Propulsion and Power*, advance, https://doi.org/10.2514/1.B36221.

[101] Hitt, M. A. and Frederick, R. A., "Testing and Modeling of a Porous Axial-Injection, End-Burning Hybrid Motor," *Journal of Propulsion and Power*, Vol. 32, No. 4, 2016, pp. 834-843, http://dx.doi.org/10.2514/1.B35939.

[102] Hitt, M. A., and Frederick, R. A., "Experimental Evaluation of a Nitrous-Oxide Axial-Injection, End-Burning Hybrid Rocket". *AIAA Journal of Propulsion and Power*, advance, https://doi.org/10.2514/1.B36439.

[103] Nagata, H., Okada, K., San'da, T., Kato, T., Akiba, R., Satori, S., and Kudo, I., "Combustion Characteristics of Fibrous Fuels for Dry Towel Hybrid Motor," *Journal of Space Technology and Science*, Vol. 13, No. 1, 1997, pp. 11-16.